

Delft University of Technology
Department of Civil Engineering
Group of Fluid Mechanics
Report No. 1783

**Selection and formulation of a
numerical shallow water wave
hindcast model**

**L.H. Holthuijsen
N. Booij**

17-83

PROJECT REPORT

**Delft University of Technology
Department of Civil Engineering
Group of Fluid Mechanics**

Project title

GEOMOR wave model

Project description

Formulate a numerical wave hindcast model which can be used to obtain realistic estimates of wave conditions in the Oosterschelde as input to a numerical geomorphological model.

Customer

Rijkswaterstaat
Deltadienst
Afdeling Kustonderzoek
Van Alkemadelaan 400
2597 AT The Hague, the Netherlands

represented by

J. van Marle

Project leader

dr.ir. L.H. Holthuijsen

work carried out by

dr.ir. L.H. Holthuijsen
dr.ir. N. Booij
T. Herbers

Conclusion

A directionally decoupled, parametric wave hindcast model is recommended that includes parameterized versions of conventional bottom- and current refraction, some degree of diffraction, and parameterized wave growth and -dissipation.

Status of report

Confidential, final report

City/date:

Delft, Nov. 30, 1983

Contents

	Page
1. Introduction	1
2. Geophysical conditions	3
3. Preliminary evaluation of wave conditions	7
3.1 Introduction	7
3.2 Wave propagation	7
3.3 Wave generation	10
4. Selection of the hindcast model	18
4.1 Introduction	18
4.2 Refraction	19
4.3 Diffraction	19
4.4 Nonlinear wave-wave interactions	21
4.5 Wind, current and bottom effects	24
5. The selected hindcast model	27
5.1 Mathematical formulation	27
5.2 Numerical formulation	44
6. Conclusion	48
References	49
Appendix	52

1. INTRODUCTION

To evaluate morphological changes in the Oosterschelde after the completion of the storm surge barrier in the entrance of the Oosterschelde, Rijkswaterstaat* has requested the Delft Hydraulics Laboratory and the Delft University of Technology to develop a numerical morphological model and two other numerical models to provide boundary conditions for this model. One of these is a tidal current model, the other is a wave hindcast model.

The wave hindcast model is the subject of the present report, that is, the selection and formulation of its basic characteristics are given. The implementation of the model on a computer is not addressed specifically.

The wave model should incorporate the phenomena of wave generation, wave dissipation and wave propagation in an area with a complex topography and a spatially variable current pattern. Fortunately, the time scales of wave propagation in the Oosterschelde are small compared with changes in wind and in tide, so that the situation can be assumed to be stationary in the calculations. On the other hand, the number of gridpoints in the model is expected to be about 20 times larger than in conventional ocean wave models, while the available computer capacity is roughly the same for both models (about 30 min CPU on a UNIVAC 1100/80). It is only by the grace of the stationarity assumption that a feasible model can be considered at all.

The method used in this study is to select a wave model by considering in sequence a number of levels at each of which state-of-the-art information is used to further eliminate potential models. At each level one physical effect is considered:

- (a) refraction
- (b) diffraction
- (c) nonlinear wave-wave interactions
- (d) wind- and bottom effects.

* Ministry of Public Works of the Netherlands

This sequence of otherwise equally important phenomena reflects an increasing degree of freedom in parameterization and thus in the numerical modelling of these phenomena. Each effect is evaluated in terms of its physical relevance for the morphological problem and in terms of its implications for required computer capacity.

The result of this elimination process is the selection of a 2-parameter model for each of a small number of spectral wave directions to be run separately for swell and for locally generated waves. The numerical implementation seems to be most efficient (in development time and to some extent also in CPU-time) when a finite difference model is used.

2. GEOPHYSICAL CONDITIONS

The Oosterschelde is located in the SW part of the Netherlands as part of the Rhine-Meuse delta (fig. 1). The surface area is about 55 km x 7 km and the orientation of its main axis is roughly WNW-ESE. It is open to the southern North Sea, permitting tide and waves to enter. In the entrance of the Oosterschelde a storm surge barrier is under construction. This barrier will change the interaction between the open sea and the Oosterschelde basin inland from the barrier. In normal conditions, the barrier will be open, reducing tide and waves moderately compared with the present situation. In severe storm conditions, the barrier will be closed.

The bottom topography in the Oosterschelde is highly irregular: a number of shoals located just below mean sea level (0-1 m), are separated from one another and from the land by tidal channels as deep as 40-50 m, fig. 2. The wave model is to be applied to each shoal separately, in particular the Roggeplaat near the entrance and the Galgeplaat further inland. Waves penetrating from the open sea will be considered as imposed boundary conditions for the wave model.

To determine the importance of various geophysical aspects of the area and of the waves, the Galgeplaat was selected by Rijkswaterstaat to be representative for the selection and development of the wave hindcast model even if the effect of waves penetrating from the open sea is more important for the Roggeplaat.

The Galgeplaat is an elongated, fairly flat shoal of approximately 12 km² surface area located at a depth of about 0.5 m below chart datum NAP (\approx mean sea level), fig. 3. It is separated from the surrounding landmass by tidal channels of 1-2 km width which are 10-40 m deep. The bottom slope around the shoal is consequently steep.

The tidal range in the present situation is from +1.75 m NAP at mean high tide to -1.75 m NAP at mean low tide. The tidal current around the Galgeplaat can be as high as 2.0-2.5 m/s at only a few hundred meters from shore, implying steep gradients in the current pattern. When the

storm surge barrier is completed these numbers will be reduced to about 1.5-2.0 m/s and + or -1.50 m for the current speed and tide level respectively.

The wind speed may vary for the wave computations from 10 to 30 m/s while the wind directions may vary from SW to N.

Wave boundary conditions for the Oosterschelde are imposed only at the entrance landward from the barrier. Here, the wave direction may vary from SW to N, the period may be as high as 6-7 s while the wave height seems to be rather modest at perhaps 0.3 m.

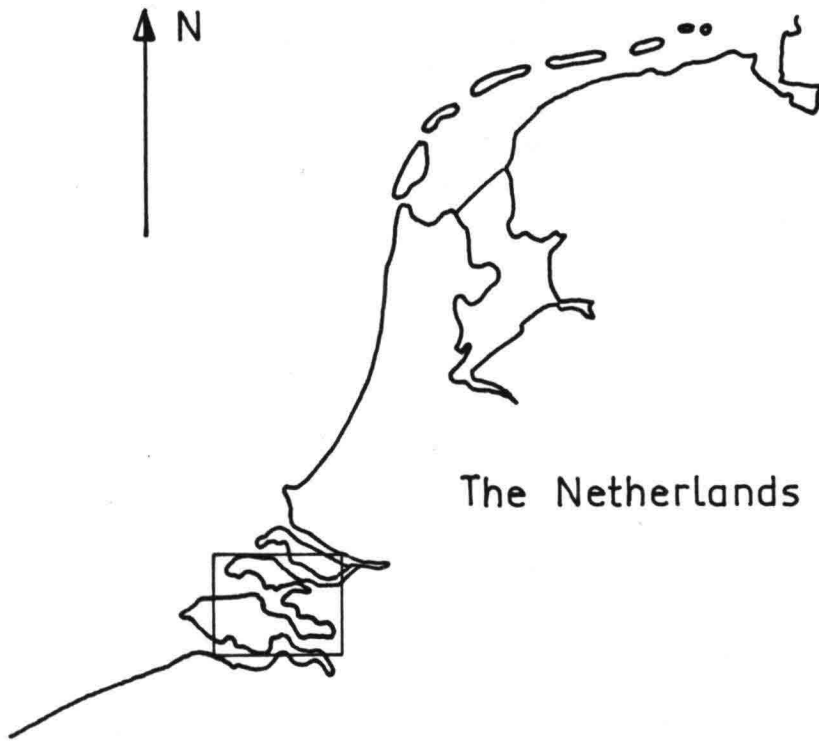


Figure 1: Location of the Oosterschelde

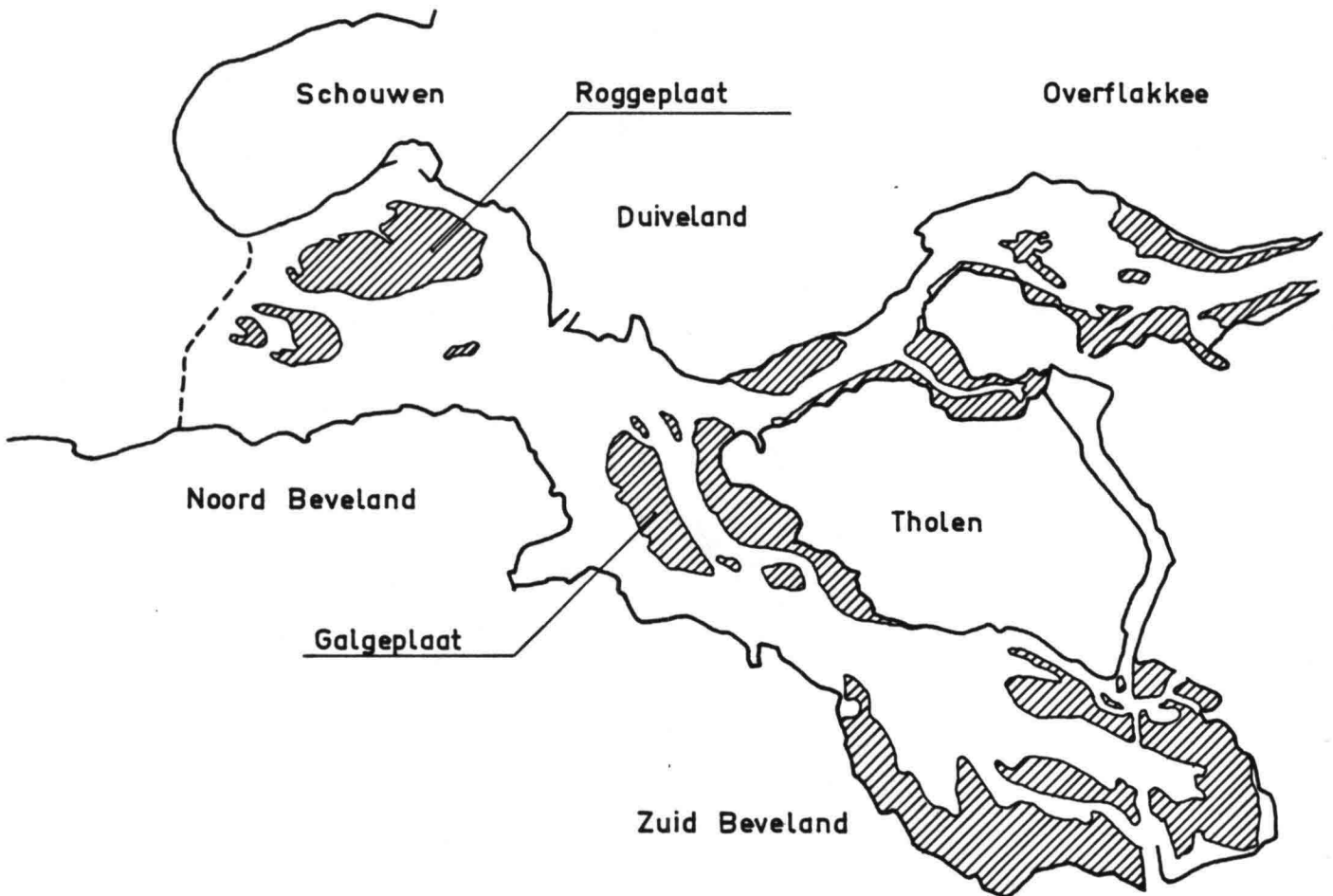


Figure 2: Tidal flats in the Oosterschelde

3. PRELIMINARY EVALUATION OF WAVE CONDITIONS

3.1 Introduction

As indicated before, four wave phenomena will be evaluated in the selection process:

- refraction
- diffraction
- nonlinear wave-wave interactions
- wind- and bottom effects.

An adequate evaluation of these phenomena would require observations in the field or in a laboratory or a highly sophisticated, well tested, numerical model. However, such observations and such a model are not available for the present study so that a rather crude approach is taken. The justification of choices made in this approach is fairly subjective. They can be substantiated only when computational results of the chosen model are confronted with observations.

The four wave phenomena can be divided into two classes: wave propagation (refraction and diffraction) and wave generation (nonlinear wave-wave interactions and wind- and bottom effects). These two classes are addressed separately in the following.

3.2 Wave propagation

In order to obtain a preliminary estimate of the effects of refraction and diffraction on the wave conditions in the Galgeplaat area, conventional bottom refraction computations have been carried out in the present study. Refraction due to current variations is not considered. It would tend to modify the wave field in a periodic manner around the situation without currents.

If the refraction computations indicate a significant effect of refraction then obviously refraction should be included in the wave model. If in addition these results indicate the existence of steep gradients in the wave energy over extended regions, then diffraction should also be included.

The results of the refraction computations can also be used to determine the degree of parameterization of the nonlinear interactions. If areas are found where wave rays intersect at fairly large angles (45° or more, say), then the occurrence of cross-seas is likely to occur in the field. Wave spectra with multi-modal directional distributions should then be considered when determining the degree of parameterization of the nonlinear wave-wave interactions.

Rijkswaterstaat provided the bottom topography of the Galgeplaat area on a grid of $50 \times 50 \text{ m}^2$ in a rectangular area of $12.5 \times 8 \text{ km}^2$, fig. 3. Note that the top of the shoal (indicated by negative numbers in fig. 3), which is located to the N from the centre of the shoal, is dry when the waterlevel is at chart datum (NAP). This area is referred to on a number of occasions in the following text. For reference a sketch is provided in figure 4.

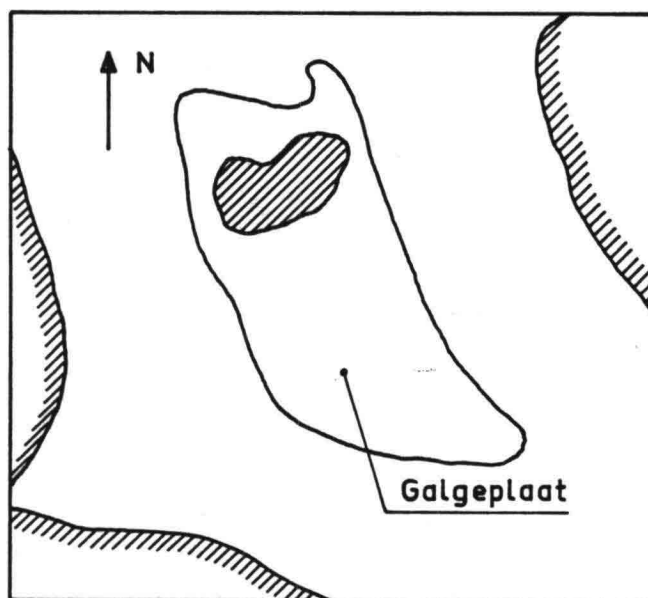


Figure 4: Approximate location of top of Galgeplaat.

The refraction computations were carried out with a ray refraction program of the group of Fluid Mechanics of the Delft University of Technology. The wave periods were chosen to be $1\frac{1}{2}$ s and 3 s. These values are based on crude estimates of the wave conditions in the Galgeplaat area in a severe storm. The maximum fetch in a storm from the NW would be about 10 km. With an average depth of 2-3 m and a constant wind speed of about 30 m/s, the significant wave period would be 2.5-3.0 s at the downwind end of the area (e.g. Shore Protection Manual, 1973). Computation with the two chosen wave periods should therefore provide a fair impression of the bottom refraction pattern in the Galgeplaat area for locally generated waves.

The Galgeplaat is most exposed to wave attack from the sector W-N from which also severe storms can be expected. Computations were therefore carried out for initial wave directions WSW, WNW, NW, NNW and NNE (wave direction at upwind boundary of bottom grid). It should be noted that for convenience of handling the input of the refraction program, rays were started only at open boundaries of the bottom depth grid. No rays were started from land boundaries. The results of the computations for the water level at NAP are given in Appendix I. An inspection of the results indicates the following.

Most of the refraction occurs at the windward side of the dry top of the shoal where these effects vary from moderate (e.g. $T = 1\frac{1}{2}$ s, NNW) to strong (e.g. $T = 3$ s, NNW). Wave rays passing on both sides of the dry top seem to do so almost undisturbed except perhaps rays from direction NW. This implies that at the leeside of the dry top the wave conditions are quiet as almost no wave energy is refracted into this area except when the initial wave direction is from around NW.

Since waves from NW seem to propagate more of their energy to the leeward side of the dry top of the shoal than do waves from the other directions, this direction is further investigated. In particular the effect of increasing the water level (e.g. to the mean tide level of +1.75 m NAP) seems to be interesting as the shoal is then completely submerged and waves propagate over the top, possibly with significant refraction effects. The results of computations for waterlevel at

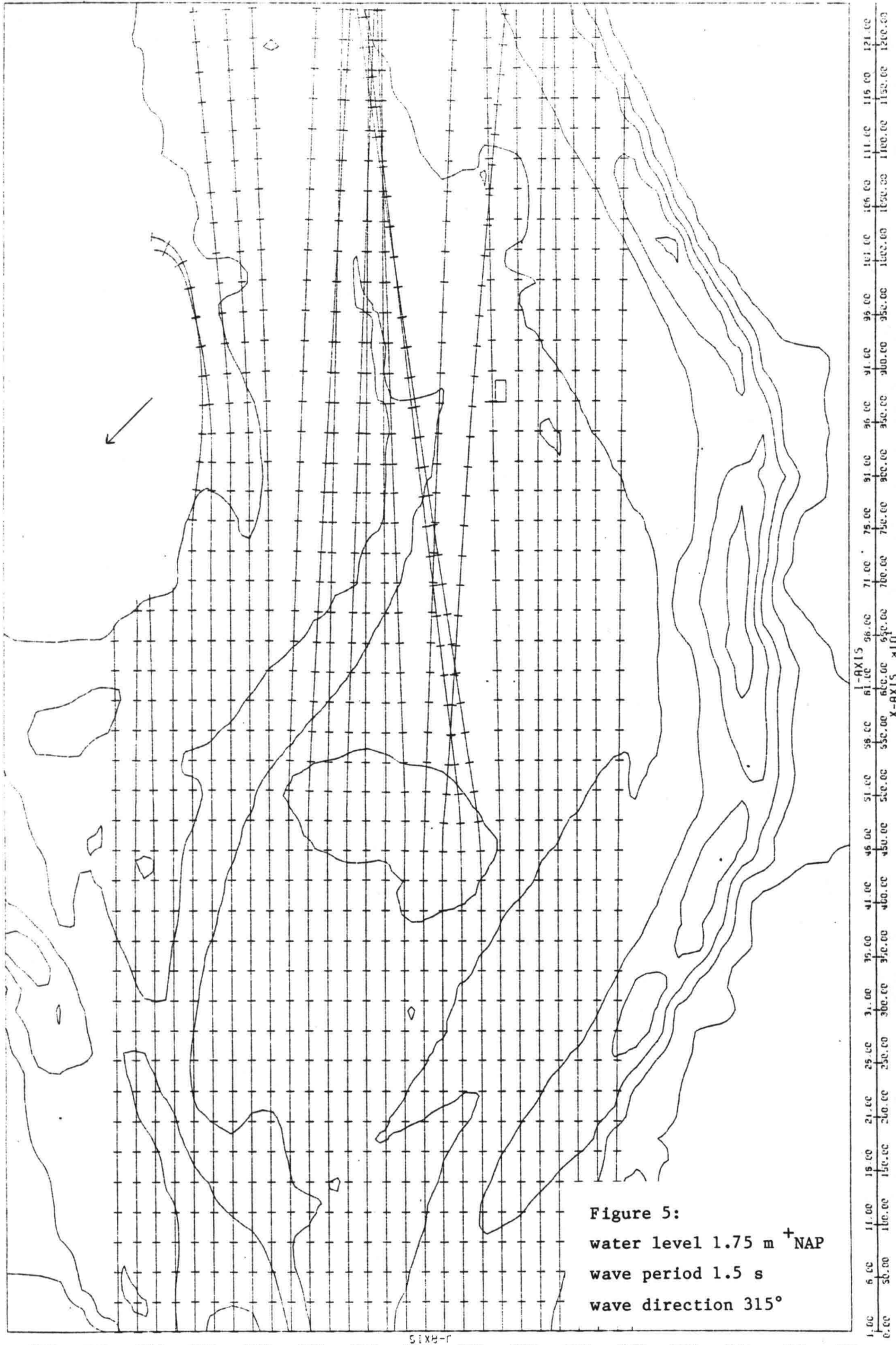
+1.75 m NAP for the periods $1\frac{1}{2}$ s and 3 s are given in figures 5 and 6. Apparently the $1\frac{1}{2}$ s waves are affected only moderately (fig. 5) but the 3 s waves produce a highly confused sea (cross seas) over the shoal at the leeward side of the top (fig. 6). The latter effect is even more dramatic for the direction NNE, fig. 7, for which a pronounced focal point is found leeward of the top.

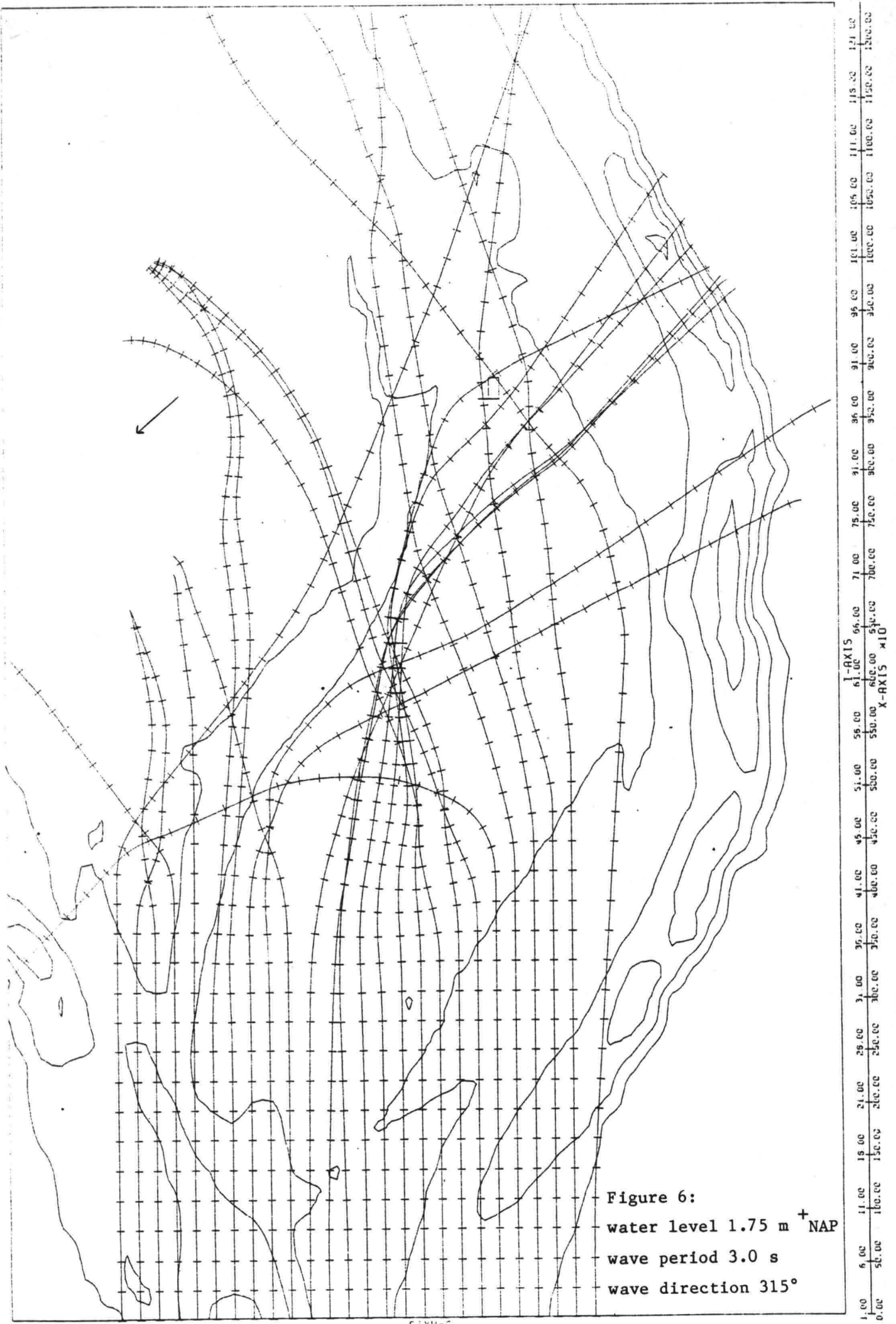
A lowering of water level lower than NAP increases the surface area of the dry top of the shoal with a corresponding decrease of wave energy at the leeward side of this dry top, fig. 8.

The main result of the above calculations is that the top of the shoal tends to focus wave energy at its leeward side for storms from north-westerly directions. The spatial distribution of the wave energy is correspondingly variable and the waves are highly confused in this area (cross-seas). It follows that refraction is significant and that probably also diffraction is significant. However, the diffraction effects may be small compared with the combined refraction of wave components from a continuum of directions (as in a spectral hindcast model). The existence of cross-seas indicates that the effects of nonlinear interactions can not be parameterized as far as they can be for ocean applications where cross-seas of growing waves do not occur.

3.3 Wave generation

As indicated before, detailed observations or a sophisticated numerical model were not available for this study to estimate wave generation. In fact, even a crude model to obtain rough estimates was not available. The relevance of the indicated processes is therefore estimated with qualitative arguments or educated guesses of the wave conditions in the Galgeplaat area outside the surfzones. Information on the situation in the surfzone is almost non-existent.





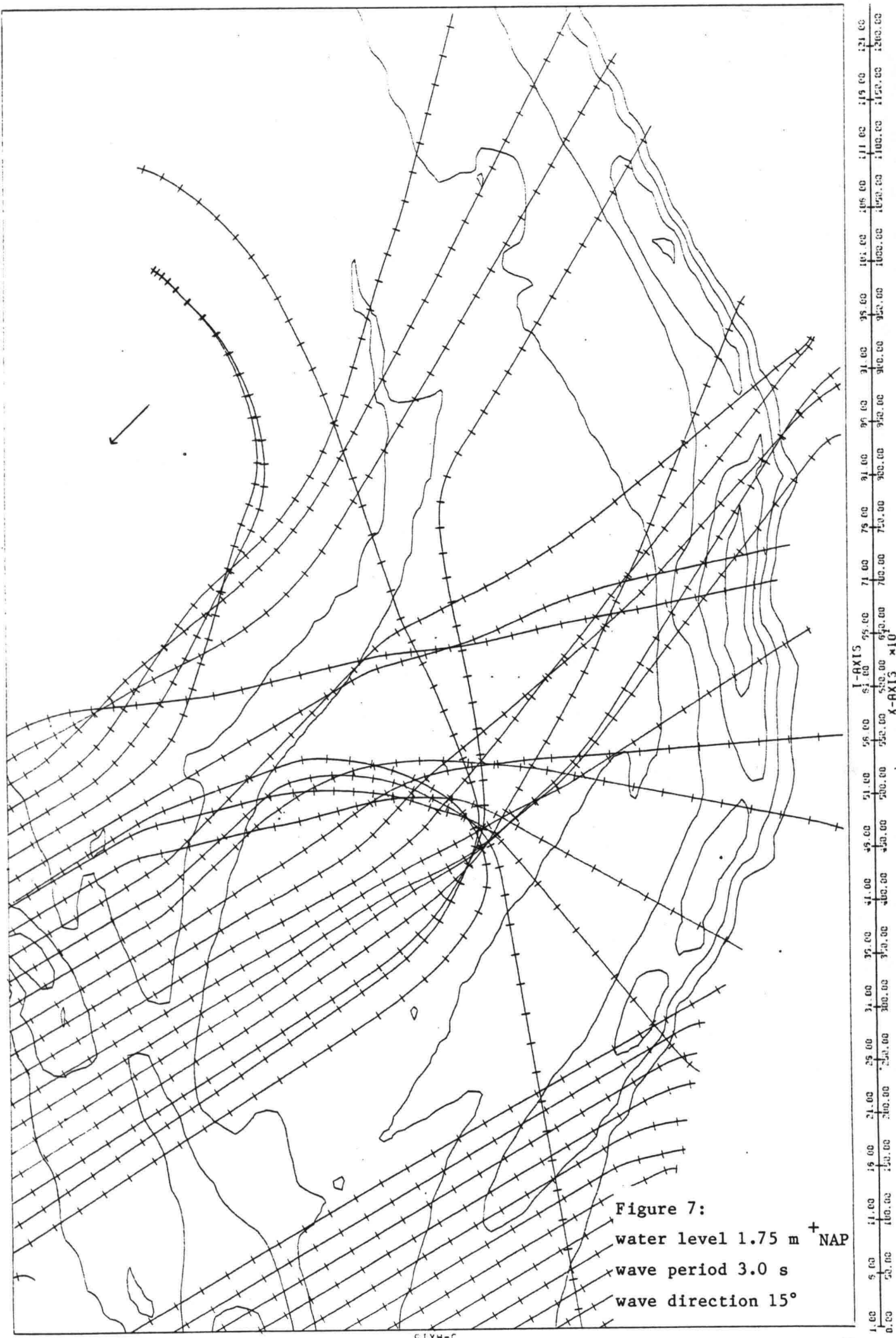


Figure 7:
water level 1.75 m + NAP
wave period 3.0 s
wave direction 15°

1.00 0.00 1.00 2.00 3.00 4.00 5.00 6.00 7.00 8.00 9.00 10.00 11.00 12.00 13.00 14.00 15.00 16.00 17.00 18.00 19.00 20.00 21.00 22.00 23.00 24.00 25.00 26.00 27.00 28.00 29.00 30.00 31.00 32.00 33.00 34.00 35.00 36.00 37.00 38.00 39.00 40.00 41.00 42.00 43.00 44.00 45.00 46.00 47.00 48.00 49.00 50.00 51.00 52.00 53.00 54.00 55.00 56.00 57.00 58.00 59.00 60.00 61.00 62.00 63.00 64.00 65.00 66.00 67.00 68.00 69.00 70.00 71.00 72.00 73.00 74.00 75.00

1.00 0.00 1.00 2.00 3.00 4.00 5.00 6.00 7.00 8.00 9.00 10.00 11.00 12.00 13.00 14.00 15.00 16.00 17.00 18.00 19.00 20.00 21.00 22.00 23.00 24.00 25.00 26.00 27.00 28.00 29.00 30.00 31.00 32.00 33.00 34.00 35.00 36.00 37.00 38.00 39.00 40.00 41.00 42.00 43.00 44.00 45.00 46.00 47.00 48.00 49.00 50.00 51.00 52.00 53.00 54.00 55.00 56.00 57.00 58.00 59.00 60.00 61.00 62.00 63.00 64.00 65.00 66.00 67.00 68.00 69.00 70.00 71.00 72.00 73.00 74.00 75.00

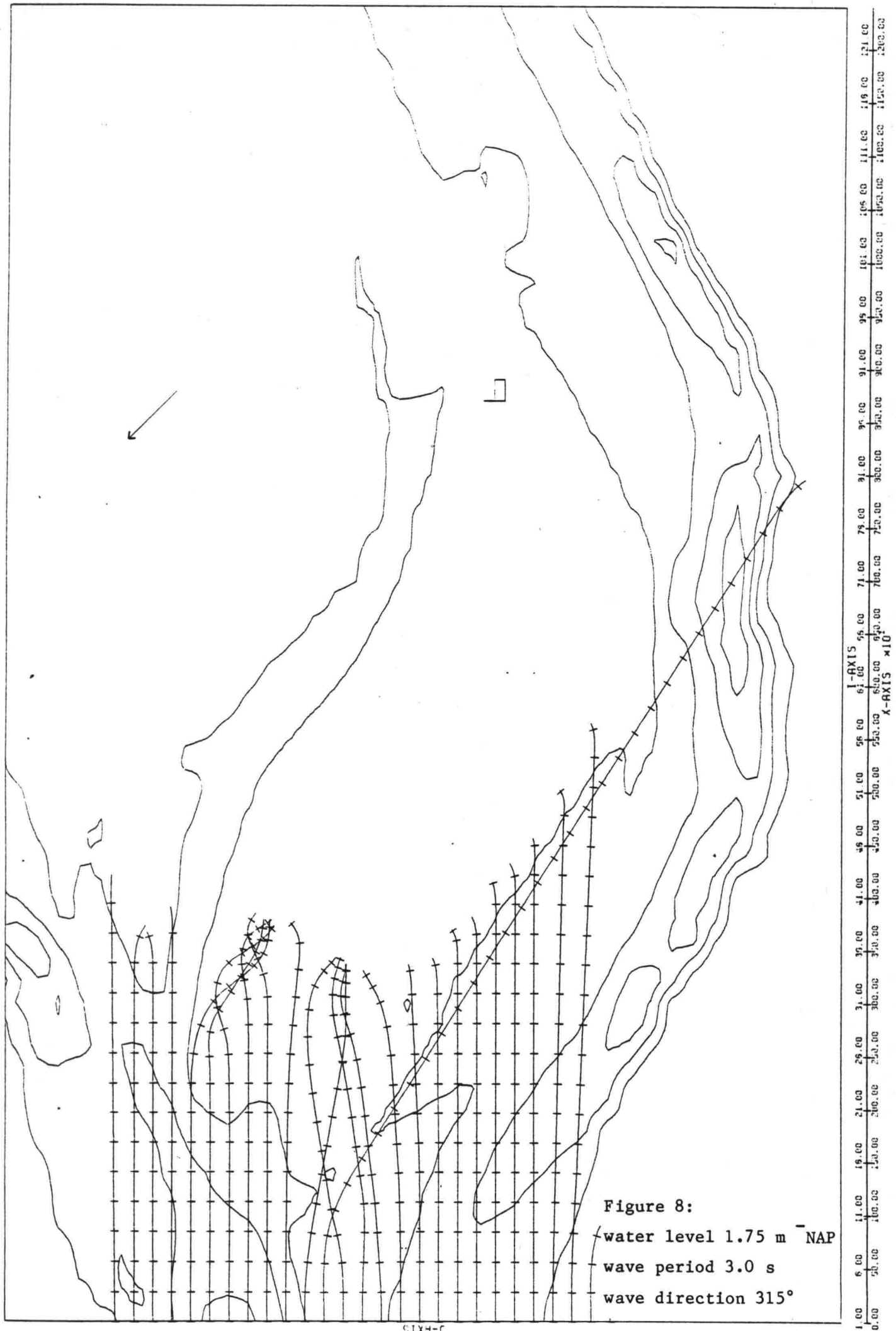


Figure 8:
water level 1.75 m ⁻NAP
wave period 3.0 s
wave direction 315°

Nonlinear wave-wave interactions

For deep water the nonlinear wave-wave interactions which are relevant for wave generation have been formulated rigorously by Hasselmann (e.g. 1968). Their effect on growing waves in deep water is to force the spectrum towards a relatively simple universal shape and also to force the relationships between the scale- and shape parameters of the spectrum on the one hand and wind on the other towards universal relationships. In situations where the wave field does not change rapidly (time and space scale in the order of a few hundred wave periods or wave lengths or more), the nonlinear interactions actually succeed in maintaining the spectrum in a universal shape and the parameters are related in a universal manner to the local wind. However, if the changes in the wave field are rapid, then such universal characteristics seem to be absent. The spectrum and the parameter relationships then only tend to develop towards these characteristics but they do not achieve them.

For shallow water situations the nonlinear interactions seem also to be significant, perhaps more so than in deep water. Again the spectrum tends to be forced into a (depth-dependent) universal shape and the spectral parameters tend to be related to the wind and the water depth in some universal manner. But these universal characteristics are probably maintained only for slowly varying wave fields.

Considering the results of the refraction computations in the previous section, one may expect the wavefield to vary slowly only in the deep water regions of the Galgeplaat area, and also for very short waves (period less than $1\frac{1}{2}$ s, say) in the shallower areas over the Galgeplaat. For these situations one may therefore expect to find universal characteristics of the wave field similar to those in deep water. However, for longer waves (period more than $1\frac{1}{2}$ s, say), the variability of the wave field seems to be high, especially over the Galgeplaat itself south of its top. Nonlinear interactions will still be important there, and they possibly dominate the development of the spectrum, but a universal spectral shape and universal parameter relationships may not be expected to hold.

Wind- and bottom effects

The wave field in the Oosterschelde basin is mostly locally generated except near the entrance where waves from the southern North Sea may penetrate. It is therefore obvious that wave generation by wind should be included in the model.

The Galgeplaat is a shallow area even when it is completely submerged at, say, mean tide level. The ratio water depth/wave length can even then be as low as $\frac{1}{2}$ to $\frac{1}{4}$. This implies that bottom effects will be important, and possibly dominant, in the shallow areas over the Galgeplaat (quite apart from shoaling, refraction and diffraction which are depth related propagation effects). The potentially most relevant bottom effects seem to be, in order of probable importance:

- wave induced turbulent bottom friction
- wave induced percolation
- back-scattering
- wave induced bottom motion.

This sequence is chosen because the bottom in the area under consideration seems to be mostly sandy. However, large parts of the Galgeplaat are covered with oyster cultures which pose unusual complications for the estimation of bottom dissipation. With the information presently available one cannot indicate whether one of the above mentioned processes dominates the others. The effect of the last process of wave induced bottom motion is probably negligible but each of the other processes may well be important, particularly if the effects of oyster cultures are considered.

Surfzone

When waves enter areas where the water depth is of the same order as the wave height (significant wave height, say), then wave breaking occurs which is different in character from breaking in deeper water. This situation of waves breaking in a surfzone will occur in the Oosterschelde basin even when the shoals are submerged. To illustrate this, consider the same wave generation situation as in the previous section on wave propagation. It was found that the maximum significant

wave period would be 2.5-3.0 s. Based on the same method of estimation and some subjective interpretation of the refraction patterns, a maximum significant wave height of about 1.0 m can be expected over the Galgeplaat. At mean high tide, the water depth at the shallowest part of the Galgeplaat is about 1.0 m, indicating that surf will appear over the Galgeplaat when the water level is at or below mean high tide.

The conclusion from the above considerations is therefore that bottom- and current refraction should be included in the hindcast model and probably also some degree of diffraction. Processes of wave generation by wind, dissipation through bottom effects and wave breaking inside the surf zone should also be included. The selection of models for these various phenomena is addressed next.

4. SELECTION OF THE HINDCAST MODEL

4.1 Introduction

The method which is used here to select the hindcast model from a large variety of potential models is essentially an elimination process: at each of four levels a different physical wave phenomenon is evaluated in terms of its physical relevance and a choice is made for a sub-model for that phenomenon. The choice at one level affects the selection of potential models at lower levels in such a way that the set of potential models reduces. This procedure is illustrated in fig. 9.

In this illustration the selected model would be a combination of the sub-models b, d, h and k. The chosen sequence of the physical phenomenon is such that the freedom of selecting a model at that level is higher than at the previous level.

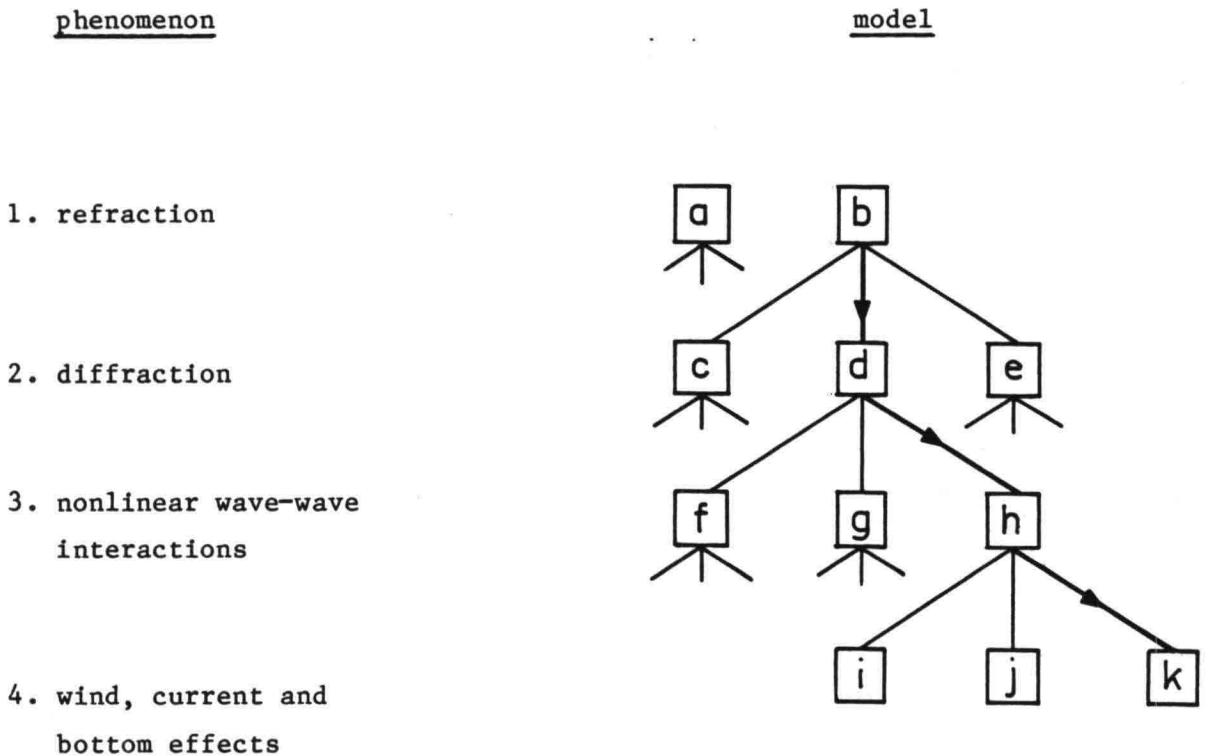


Figure 9: Selection process for the hindcast model.

4.2 Refraction

Considering the results of the refraction computations given in the previous section it is obvious that bottom refraction should be included in the model. Also current refraction can be expected to be significant in view of the steep gradients in the tidal currents in the Oosterschelde.

The freedom in selecting a refraction model is limited: either a conventional refraction model is used or not. This implies that only the numerical implementation is free to be chosen. From a numerical point of view two models can be implemented: propagation of wave energy along wave rays or over a regular grid. The first approach is conventional (e.g. Whitham, 1974), the second would be less so. It seems that in terms of CPU-time the two models would be equally expensive: about 1 sec on a UNIVAC 1100 to propagate wave energy at one frequency and one initial direction from the north end of the Galgeplaat area to the south end with a resolution of $50 \times 50 \text{ m}^2$.

The wave ray model has the disadvantage that for the calculation of nonlinear phenomena (e.g. wave breaking) and for the output of results, the information from different rays within each bin of the grid needs to be integrated over that bin. One can conceivably use for this the method of Bouws and Battjes (1978) but the repeated transformation from grid to ray and back would add considerable CPU-time to the computations. It is therefore recommended that the refraction computations be carried out on a regular grid (where such transformation do not occur). A version in which the computations propagate with the wave crests seems to be computationally efficient. This approach would be similar to the one used in the CREDIZ-model of Rijkswaterstaat (Booij and Radder, 1981). The mathematical and numerical formulations are given in section 5.

4.3 Diffraction

The occurrence of regions with steep gradients in wave energy in the results of the refraction computations of section 3.2 indicates that

diffraction is probably important over the Galgeplaat. However, these computations were carried out for one frequency and one initial wave direction for each plotted ray pattern. This distorts, at least to some extent the impression of the actual situation in which a continuum of frequencies and directions should be considered. The spatial wave energy distribution is therefore smoother in the field than refraction computations for one frequency and one direction suggest. To what extent this smoothing suppresses the need of diffraction in the hindcast model has not been investigated since such an evaluation requires a model in which diffraction can be suppressed or activated at will. Such a model is not available for the present study. An alternative would be to combine the results of a limited number of refraction computations to evaluate the then resulting gradients in the energy distribution. But this was considered to be outside the scope of this study. It is therefore recommended to include in the hindcast model a fairly flexible diffraction representation. Its physical relevance can be evaluated in the calibration phase of the model.

The mathematical formulation of diffraction in an area with mild bottom slopes has been given by Schönfeld (1972) and Berkhoff (1976). The result is referred to as the mild slope equation which also includes refraction. An earlier, but incomplete version has been given by Battjes (1968). The application of the mild slope equation for any operational problem is prohibitively expensive in terms of required computer effort. Firstly, it requires a high resolution in the horizontal plane (a small fraction of the wave length) and, secondly, the equation is of the elliptic type which implies a large number of iterations or the inversion of a large matrix. A more efficient approach is found in an alternative to the mild slope equation. It involves a parabolic approximation of the mild slope equation in which diffraction effects in the direction of wave propagation are neglected. In this approach the wave field can be computed directly per grid point with considerably less effort than in the above approach. This parabolic approximation has been used in the CREDIZ model of Rijkswaterstaat. However, the required computer effort would still be excessive due to the high resolution which is the same as for the mild slope equation.

The qualification of excessive computer effort is based on an estimated CPU-time per frequency, direction combination, and an assumed large number of such combinations (a discrete spectral approach to wave hindcasting). An alternative to this discrete spectral approach is to parameterize the wave field with only 3 parameters (frequency, direction and wave height) which may each vary in the horizontal plane. If such a parameterization is accepted one might argue that the CREDIZ model can be modified to accommodate a wave period and wave height which vary in the horizontal plane due to wind, current and bottom effects. Two objections to such an approach are given here:

- (a) such spatial variations of frequency in CREDIZ would result in a spatial variation in phase speed which are not due to current- and depth variations. The corresponding refraction would consequently be spurious.
- (b) the required resolution in the horizontal plane would still be high and CPU-time would be excessive.

It is therefore recommended for the hindcast model to have a fairly primitive sub-model for diffraction. Such a sub-model could be represented as a propagation term in the energy balance equation of the waves to transport energy in the dimensions of wave directions in the spectral plane. If the relevant propagation speed in this term would depend on spatial energy gradients, then such a term would result in a diffraction-type transport across spatial wave energy gradients. A more primitive approach would be to include in the energy balance equation a term to diffuse wave energy over the horizontal plane.

The above suggestions to model diffraction require further consideration but this is deemed to be outside the scope of the present study. The mathematical and numerical formulation of diffraction is given in section 5.

4.4 Nonlinear wave-wave interactions

As indicated earlier, the importance of nonlinear wave-wave interactions is found in their domination of the development of the wave spectrum by a redistribution of the wave energy within the spectrum. This has been demonstrated theoretically and empirically in deep water (e.g. Hasselmann et al., 1973; Houmb et al., 1976).

For wave fields which vary rapidly in space or time the nonlinear interactions do not seem to succeed in maintaining a universal spectral shape and universal relationships between spectral parameters. This would imply that these interactions need to be represented explicitly in a discrete spectral energy balance. Such a model would probably give the most reliable hindcast results. However, this would be excessively expensive in terms of development effort and CPU-time, even when the interactions are represented in a highly simplified manner. The estimated CPU-time for such a discrete spectral model with a highly simplified representation of the nonlinear interactions would still be on the order of 2 hours, on a UNIVAC 1100/80 for one stationary situation over the Galgeplaat area. This is prohibitive and one is therefore forced to assume some universal character of the wave spectrum so that this spectrum can be parameterized at least to some degree. In that case, only the parameters of this spectrum need be hindcasted with a relatively small number of (coupled) equations (one for each of the parameters).

Two types of parameterization can be suggested. One is to decouple the frequencies and to assume a universal directional distribution per frequency, the other is to decouple the directions and to assume a universal frequency distribution per direction. The choice between these two alternatives seem to be determined by the spatial variability of either the directional characteristics or of the frequency characteristics of the spectrum.

The results of the refraction computations suggest through the occurrence of cross-seas that at least the directional characteristics of the spectrum can vary considerably over the Galgeplaat. Although corresponding calculations have not been made to estimate the spatial variability of the frequency characteristics of the spectrum, a subjective expectation is that this variability is less than that of the directional characteristics. The conclusion from this is that, if the spectrum has to be parameterized, it is better to parameterize the frequency distribution (per direction) than to parameterize the directional distribution (per frequency): a directionally decoupled model is recommended.

Although one parameter per direction may be enough to obtain realistic hindcast results in deep water it is felt that for shallow water at least two parameters per direction are needed. The suggested parameters are the frequency-integrated energy density E_0 and a mean frequency ω_0 (section 5).

The CPU-time for such a model with 8 directions say (a 16 parameter model), would be roughly 30 min on a UNIVAC 1100/80 for one stationary situation over the Galgeplaat. This is also the maximum CPU-time permitted by Rijkswaterstaat for the operational use of the model.

A further parameterization could be achieved by parameterizing the entire wave spectrum with a small number of parameters e.g. a total energy, a characteristic frequency and a characteristic direction (a 3-parameter model in which the frequencies and directions are coupled). Such a model is not recommended for the following two reasons.

(1) Tunneling effect. In areas where the directional distribution of the wave energy is uni-modal the 3-parameter model may perform reasonably well. However, when the waves enter an area of energy concentration with cross-seas, the actual directional characteristics of the wave are poorly represented by a 3-parameter model. The model allows only one wave direction in each point. One important effect of this is that the modelled wave propagation is unrealistic: the wave direction will be equal to some weighted average of the actual wave directions in a point. The wave energy in the model propagates in that average direction and it therefore remains fairly concentrated in a narrow beam downwind from the area of energy concentration ("tunnel"). A model with decoupled directions will provide a more realistic representation of the directional characteristics, which spreads the wave energy after passing through the area of energy concentration (fig. 10).

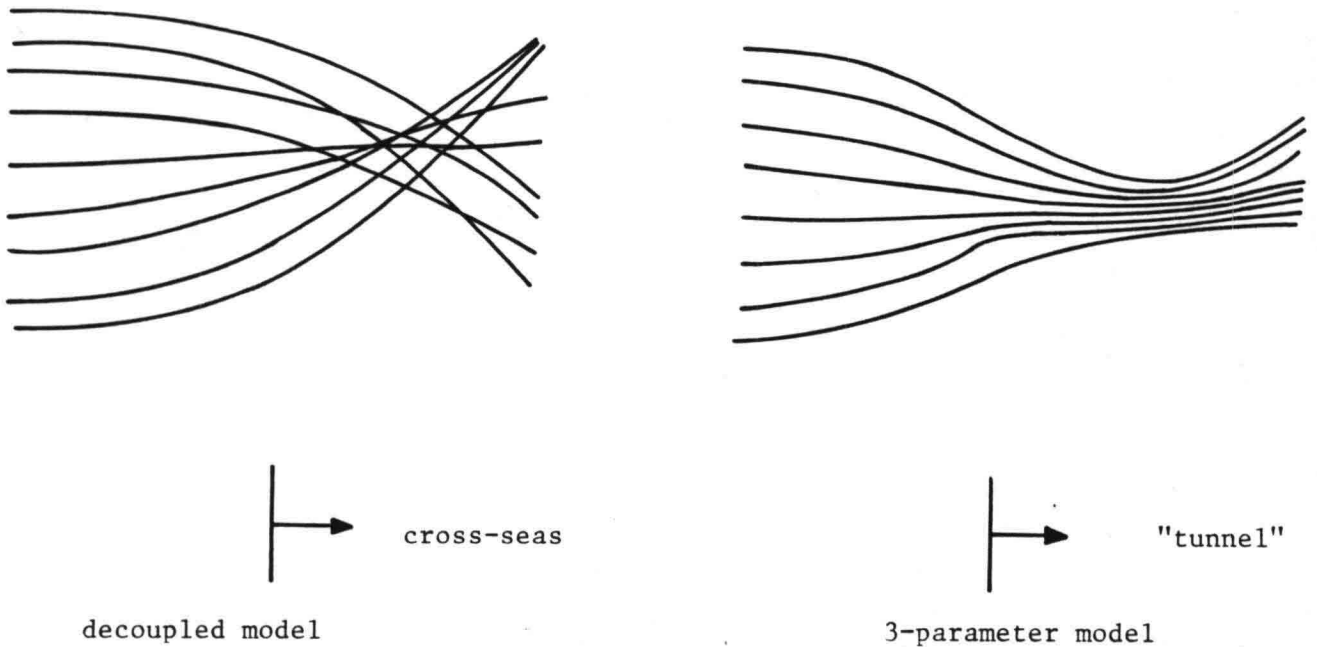


Figure 10: The propagation of wave-energy in a directionally decoupled model and a directionally coupled model.

- (2) Boundary effects. The development of waves near a coast is affected by the presence of such a coast. This presence can be accounted for by considering the distance (from the point of hindcast) to the coast as a function of direction. In the directionally decoupled model such effects are readily taken into account. In the 3-parameter model such effects can only be modelled through rather ad-hoc assumptions, which depend on the actual geometry of the coastline under consideration. This is operationally cumbersome and therefore not desired.

4.5 Wind, current and bottom effects

The freedom in choosing models to represent the effects of wind, current and bottom is potentially large. But the selections at the previous levels of the sub-models for refraction, diffraction and nonlinear wave-wave interactions have limited this freedom to some extent. In particular the decisions to couple the frequencies and to decouple the directions in the wave spectrum implies that discrete spectral representations of the wind, current and bottom effects need

not be considered (that is: for each combination of frequency and direction separately).

A convenient, and fairly common sub-model to represent the growth of the significant wave height due to wind action is based on universal relationship between the growth rate of this wave height on the one hand and the local wave height and the local wind speed on the other (e.g. Wilson, 1955; Sanders, 1976; Klatter, 1983). Such a model can be readily formulated also for the significant wave period. These sub-models can be applied directly to the 3-parameter model indicated earlier. For application in the directionally decoupled model one can supplement the above universal relationships with a directional character. Such an extension seems to be adequate for the present purpose.

The effect of currents on the generation of wave energy is not well studied. It seems therefore that for implementing such effects in the hindcast model, a pragmatic approach is required. Using the local wind vector relative to the local current vector instead of the local wind vector alone seems to be acceptable to represent the effects of currents in the hindcast model.

It seems consistent with the parameterization of the wind induced growth of the waves as described above, to represent the bottom effects by using a conventional bottom friction model formulated in terms of the two parameters for each of the spectral directions.

Inside the surfzone the development of the wave field is dominated by breaking of the waves. To determine the corresponding energy dissipation the model suggested by Battjes and Jansen (1978) seems to be adequate. This model provides only an estimate of the total energy dissipation in the surfzone, it does not give a distribution of this dissipation over directions. Since visual observations in the laboratory and on the beach seem to indicate that individual breaking waves maintain their individual direction during breaking when they cross, it is recommended here to distribute the energy dissipation proportional to the directional energy density, at least during the

early development of the hindcast model. When more information comes available (test runs, observations) another dissipation distribution may be implemented.

No information seems to be available on the frequency characteristics of the energy dissipation in the surfzone. A change in characteristic frequency of the waves seems to be very well possible. Due to the lack of information a simple relationship between the energy dissipation on the one hand and the rate of change of the significant wave period seems to be adequate, at least during the initial phase of the development of the hindcast model.

5. THE SELECTED HINDCAST MODEL

The model which has been selected in the previous section needs to be formulated in mathematical terms before an adequate numerical model can be formulated. This formulation is given here in roughly the same sequence as used in the selection process: the description of refraction and diffraction is followed by the description of wave generation and dissipation. The effects of currents are addressed separately.

5.1 Mathematical formulation

Propagation

To describe refraction and diffraction, the sea surface is first considered as a harmonic wave subject to the linear theory of surface gravity waves. The theoretical results for this type of wave are then used to transform the spectral energy balance equation into conservation equations for the previously chosen spectral parameters E_0 and ω_0 .

Refraction

The surface elevation of a wave which is harmonic and stationary in time can be written as

$$h(\underline{x}, t) = \text{Re}\{a(\underline{x})e^{i(\psi(\underline{x}) - \omega t)}\} \quad (1)$$

in which h is the surface elevation relative to its mean, \underline{x} is the horizontal coordinate $\underline{x}=(x,y)$, a is amplitude, ψ is phase, ω is frequency and t is time. The spatial variations of the wave are thus represented by the spatial variations in amplitude a and phase ψ . The latter may be loosely interpreted as representing the pattern of wave crests in the horizontal plane.

The conventional theory for refraction (e.g. Whitham, 1974) states that the phase function ψ can be found from:

$$|\nabla\psi|^2 = k^2 \quad (2)$$

in which k is the wavenumber obtained from the dispersion relationship

$$\omega = \{gk \tanh(kd)\}^{\frac{1}{2}} \quad (3)$$

in which d is the local water depth. The equation (2) thus determines the propagation of wave energy. It is a partial differential equation of first order for which solutions with characteristics exist. The characteristics for this equation are curved lines in $(\underline{x}, t, \underline{k}, \omega)$ -space which are conventionally called wave rays. In stationary situations these characteristics are determined by

$$\frac{dx_i}{dt} = \frac{c}{k} \nabla_i \psi \quad i = 1, 2 \quad (4)$$

$$\frac{d}{dt} (\nabla_i \psi) = - \frac{\partial \omega}{\partial d} \nabla_i d \quad (5)$$

in which c is the speed of wave energy propagation (group velocity) defined as

$$c = \frac{\partial \omega}{\partial k} \quad (6)$$

the two horizontal components of \underline{x} are $x_1 = x$ and $x_2 = y$; ∇_i is the gradient in either x - or y - direction. If the direction of the vector $\nabla\psi$ in the (x,y) -plane is denoted by θ , it follows from (4) that θ is also the direction of the ray. Due to (2) the ray equations (4) can be simplified to:

$$\left. \begin{aligned} \frac{dx}{dt} &= c \cos \theta \\ \frac{dy}{dt} &= c \sin \theta \end{aligned} \right\} \quad (7)$$

The rate of change of θ when travelling along the wave ray with speed c can be derived from (5):

$$\begin{aligned}
 \frac{d\theta}{dt} &= \frac{1}{k} \frac{\partial \omega}{\partial d} \left\{ -\frac{\partial x}{\partial d} \sin\theta + \frac{\partial d}{\partial y} \cos\theta \right\} \\
 &= -\frac{1}{k} \frac{\partial \omega}{\partial d} \frac{\partial d}{\partial n} \\
 &= \frac{c}{k} \frac{\partial k}{\partial n}
 \end{aligned} \tag{8}$$

in which $\partial/\partial n$ is the gradient in the direction orthogonal to θ . Since the wavenumber k can be determined from (3) for every \underline{x} , the position of the ray can be calculated from (7) and (8) for given initial values of \underline{x} and θ .

The above formulation is fairly conventional in the literature on refraction. However, in hindcast models, the variables \underline{x} , t , \underline{k} and ω are usually not treated as dependent variables but as independent variables. The notion of tracking wave energy through $(\underline{x}, t, \underline{k}, \omega)$ -space along wave rays is abandoned. Instead, propagation of wave energy is considered locally for every $(\underline{x}, t, \underline{k}, \omega)$ -combination. These variables are then independent variables and the wave energy is a dependent variable in the six-dimensional $(\underline{x}, t, \underline{k}, \omega)$ -space. Due to the dispersion relationship (3) the wave energy is located on a curved surface in (\underline{k}, ω) -space. This implies that the three dimensions of (\underline{k}, ω) can be reduced to two in the model. For the model (ω, θ) will be chosen for these two dimensions. In addition, time t is only an auxiliary variable for a stationary situation so that this dimension can also be dropped as an independent variable. The result of these reductions is that it is sufficient to distribute the wave energy over the four-dimensional $(\underline{x}, \omega, \theta)$ -space. The corresponding wave energy density per unit surface area per unit frequency per unit direction is denoted as E :

$$E = E(\underline{x}, \omega, \theta) \tag{9}$$

The effects of wave propagation, generation and dissipation, in other words the hindcasting of E , is normally based on the energy balanced equation:

$$\frac{\partial}{\partial x} \left(\frac{dx}{dt} E \right) + \frac{\partial}{\partial y} \left(\frac{dy}{dt} E \right) + \frac{\partial}{\partial \theta} \left(\frac{d\theta}{dt} E \right) + \frac{\partial}{\partial \omega} \left(\frac{d\omega}{dt} E \right) = S \tag{10}$$

The terms dx/dt and dy/dt are the x- and y-components of the energy transport speed c respectively. They will be denoted by c_x and c_y . The rate of propagation in θ -space (rate of directional shift) is $d\theta/dt$ which will be denoted by c_θ .

$$\left. \begin{aligned} c &= c \cos\theta \\ c &= c \sin\theta \\ c_\theta &= \frac{d\theta}{dt} \end{aligned} \right\} \quad (11)$$

The righthand side of (10) is the source term S which is the local rate of change of E induced by wind or bottom effects. Since frequency ω is constant, $d\omega/dt = 0$. The energy balance can then be written as:

$$\frac{\partial}{\partial x} (c_x E) + \frac{\partial}{\partial y} (c_y E) + \frac{\partial}{\partial \theta} (c_\theta E) = S \quad (12)$$

This equation (12) is also a first order partial differential equation; its characteristics are determined by (7) and (8). The first two terms in the equation represent locally linear propagation in (x,y)-space (as in water of constant depth), the third term represents the refraction effects.

Diffraction

It was indicated in section 4 that the inclusion of diffraction in the hindcast model may or may not be required. The reason for this uncertainty is the lack of quantitative information on this phenomenon in the area under consideration. A flexible and pragmatic approach to modelling diffraction was therefore recommended.

A mathematically correct representation of diffraction in the spectral energy balance equation seems to be well possible. This will be demonstrated first. However, the implementation in a hindcast model seems to require considerable effort. Two ad hoc alternatives are therefore given to include diffraction-like effects in the hindcast model.

In an area with relatively mild bottom slopes one can formally describe wave propagation (including both refraction and diffraction) with the mild-slope equation of Berkhoff (1976), ignoring wave generation and dissipation:

$$\nabla(c'c \nabla \tilde{h}) + k^2 c'c \tilde{h} = 0 \quad (13)$$

in which

$$\tilde{h}(\underline{x}) = a(\underline{x}) e^{i\psi(\underline{x})} \quad (14)$$

and the phase speed c' is

$$c' = \frac{\omega}{k} \quad (15)$$

Substituting (14) in (13) one finds for phase function $\psi(\underline{x})$:

$$|\nabla\psi|^2 = k^2 + \frac{\nabla(c'c \nabla a)}{c'ca} \quad (16)$$

in which k is determined by the dispersion relationship (3).

Comparing (16) with (2) shows that the first term on the righthand side of (16), or more precisely its gradient, represents refraction and that the second term represents diffraction. If the second term on the righthand side of equation (16) is assumed to be known as a function of x and y , then diffraction can be readily included in the model by using (16) rather than (2) in determining the characteristic equations. The effect on the energy balance equation would be a modification of the rate of directional shift. Denoting this modified shift rate as c_{θ}^* , the energy balance equation is written in analogy with (12) as:

$$\frac{\partial}{\partial x} (c_x E) + \frac{\partial}{\partial y} (c_y E) + \frac{\partial}{\partial \theta} (c_{\theta}^* E) = S \quad (17)$$

In analogy with (8) the modified rate of directional shift c_{θ}^* is given by:

$$c_{\theta}^* = \frac{c}{k} \frac{\partial k}{\partial n} \quad (18)$$

in which

$$k^* = \left\{ k^2 + \frac{\nabla(c'c\nabla a)}{c'ca} \right\}^{\frac{1}{2}} \quad (19)$$

The difference between the refraction induced c_θ and c_θ^* which is induced by both refraction and diffraction is essentially the second term on the righthand side of this equation (19). If no amplitude variation would occur, then this term would reduce to zero and the expression for c_θ^* would reduce to that for refraction.

Unfortunately the diffraction effects are formulated above, as in the theory of Berkhoff (1976), in terms of a wave amplitude which cannot be defined in terms of spectral parameters. This renders expression (19) unsuitable for applications in the spectral balance equation (17). A continued investigation at this point is therefore required to formulate the theory of Berkhoff (1976) in terms of a two-dimensional energy density. Such a reformulation is deemed to be outside the scope of the present study. However, one important conclusion from the above can be used without great effort. Apparently diffraction can be modelled as a modification of the directional shift velocity c_θ . A pragmatic alternative to the above formal approach seems therefore to use a simpler, ad hoc modification of c_θ . It should have the desired property of propagating wave energy across spatial gradients in the energy distribution in the (x,y)-plane.

One alternative seems to be a modification of c_θ which depends on the spatial gradient of the energy density normal to the direction of propagation,

$$\frac{\partial}{\partial x}(c_x E) + \frac{\partial}{\partial y}(c_y E) + \frac{\partial}{\partial \theta} \left\{ c_\theta E + \alpha \left(c_y \frac{\partial E}{\partial x} - c_x \frac{\partial E}{\partial y} \right) \right\} = S \quad (20)$$

in which α is a dimensionless number to be determined empirically.

Still another approach to simulate diffraction, but cruder than the one above, is to diffuse the wave energy in the (x,y)-domain or in the (θ)-domain. This is readily modelled by adding a diffusion term to the spectral energy balance. For diffusion in the (x,y)-domain:

$$\frac{\partial}{\partial x}(c_x E - D_x \frac{\partial E}{\partial x}) + \frac{\partial}{\partial y}(c_y E - D_y \frac{\partial E}{\partial y}) + \frac{\partial}{\partial \theta}(c_\theta E) = S \quad (21)$$

or, for diffusion in the (θ) -domain:

$$\frac{\partial}{\partial x}(c_x E) + \frac{\partial}{\partial y}(c_y E) + \frac{\partial}{\partial \theta}(c_\theta E - D_\theta \frac{\partial E}{\partial \theta}) = S \quad (22)$$

The values of the diffusion coefficients D_x , D_y and D_θ would have to be determined empirically.

Currents

The effects of currents on the propagation of wave energy has been ignored in the above. They will be addressed in the following as corrections on the above expressions for refraction, using the same sequence and the same definitions. The effects of currents on diffraction can probably be treated in a manner analogous to the one used above with an expansion based on the theory of Booij (1981). The corresponding mathematical formulations are not investigated here as these are deemed to be outside the scope of this study.

For refraction the following modifications to the original equations apply. The dispersion relationship (3) should be modified to read

$$\sigma \equiv \omega - \underline{k} \cdot \underline{U} = \{gk \tanh(kd)\}^{\frac{1}{2}} \quad (23)$$

in which \underline{U} is the current vector, ω is the absolute frequency (in a frame of reference fixed to the bottom) and σ is the relative frequency (in a frame of reference travelling with velocity \underline{U}). The corresponding effects on the wave propagation are extra terms in the expressions for the characteristics (4) and (5),

$$\frac{\partial x_i}{\partial t} = c \frac{\nabla_i \psi}{|\nabla \psi|} + U_i \quad (24)$$

$$\frac{\partial}{\partial t}(\nabla_i \psi) = - \frac{\partial \sigma}{\partial d} \nabla_i d - \sum_{j=1}^2 k_j \frac{\partial U_j}{\partial x_i} \quad (25)$$

Again θ is the direction of the vector $\nabla_i \psi$. It is no longer the direction of the characteristic (along which the energy propagates with

speed dx_1/dt) because of the "offset" given by U_1 in (24). The directional shift velocity is, in analogy with (8),

$$\frac{d\theta}{dt} = -\frac{1}{k} \frac{\partial \sigma}{\partial d} \frac{\partial d}{\partial n} - \frac{1}{k} \sum_{j=1}^2 k_j \frac{\partial U_j}{\partial n} \quad (26)$$

It seems logical to continue the present line of reasoning with introducing these modified velocities of (24) and (26) into the energy balance equation. However, energy is no longer conserved in the wave field in the presence of currents. Instead it is wave action that is conserved (e.g. Bretherton and Garrett, 1969; Whitham, 1971). In a manner analogous to the definition of energy density, wave action density is defined as function of frequency and direction:

$$A(\omega, \theta) \equiv \frac{E(\omega, \theta)}{\sigma} \quad (27)$$

The basis of the hindcast model is consequently not the energy balance equation but the action balance equation

$$\frac{\partial}{\partial x} (c_x A) + \frac{\partial}{\partial y} (c_y A) + \frac{\partial}{\partial \theta} (c_\theta A) = \frac{S}{\sigma} \quad (28)$$

in which

$$\left. \begin{aligned} c_x &= c \cos\theta + U_x \\ c_y &= c \sin\theta + U_y \\ c_\theta &= \frac{d\theta}{dt} \end{aligned} \right\} \quad (29)$$

with c from (6) and $d\theta/dt$ from (26).

Parameterization

A straightforward approach to numerically implement the action balance equation in a wave hindcast model would be to transform equation (28) into a finite difference model. However, in the previous section it has been argued that a finite difference model for each individual wave component (ω, θ) would be prohibitively expensive in the present context. Instead a parametric approach was recommended.

The parameters E_0 and ω_0 which were chosen to replace the spectral energy density are just as irrelevant as E in the hindcast model when currents are present. The two corresponding action parameters are a frequency-integrated action and a mean action frequency,

$$A_0(x, y, \theta) = \int_0^{\infty} A(x, y, \omega, \theta) d\omega \quad (30)$$

$$\omega'_0(x, y, \theta) = \int_0^{\infty} \omega A(x, y, \omega, \theta) d\omega \quad (31)$$

The corresponding conservation equations can be obtained from the spectral action balance equation (28) by applying to this equation the same operators as used in the definition of A_0 and ω'_0 . The results are (diffraction excluded):

To determine action density A_0 :

$$\int_0^{\infty} \left[\frac{\partial}{\partial x} (c_x A) + \frac{\partial}{\partial y} (c_y A) + \frac{\partial}{\partial \theta} (c_\theta A) \right] d\omega = \int_0^{\infty} \frac{S}{\sigma} d\omega \quad (32)$$

If it is assumed that

$$\int_0^{\infty} c A d\omega \simeq c'_0 A_0 \quad (33)$$

in which c'_0 is the group velocity at the mean action frequency ω'_0 , then (32) can be written as

$$\frac{\partial}{\partial x} (c'_{x0} A_0) + \frac{\partial}{\partial y} (c'_{y0} A_0) + \frac{\partial}{\partial \theta} (c'_{\theta 0} A_0) \simeq \int_0^{\infty} \frac{S}{\sigma} d\omega \quad (34)$$

in which

$$c'_{\theta 0} = -\frac{1}{k_0} \left(\frac{\partial \sigma}{\partial d} \right)_0 \frac{\partial d}{\partial n} - \frac{1}{k_0} \sum_{j=1}^2 k_{0j} \frac{\partial U_j}{\partial n} \quad (35)$$

in which k_0 is the wavenumber from equation (23) corresponding to ω'_0 and $(\partial \sigma / \partial d)_0$ is the derivative of σ for constant value k (corresponding to σ_0 in equation 23).

To determine the mean action frequency ω'_0 :

$$\int_0^{\infty} \omega \left[\frac{\partial}{\partial x}(c_x A) + \frac{\partial}{\partial y}(c_y A) + \frac{\partial}{\partial \theta}(c_\theta A) \right] d\omega = \int_0^{\infty} \omega \frac{S}{\sigma} d\omega \quad (36)$$

If it is assumed that

$$\int_0^{\infty} \omega c A d\omega \approx \omega'_0 c'_0 A_0 \quad (37)$$

and if $\underline{k} \cdot \underline{U}$ is small compared with ω , then the righthand side of (36) can be approximated as

$$\int_0^{\infty} \omega \frac{S}{\sigma} d\omega \approx \frac{\omega'_0 S_0}{\sigma_0} \quad (38)$$

in which ω'_0 is the mean absolute frequency of the action density spectrum,

$$\omega'_0 = \frac{\int_0^{\infty} \omega A(\omega) d\omega}{\int_0^{\infty} A(\omega) d\omega} \quad (39)$$

and σ_0 is the mean relative frequency of the action density spectrum,

$$\sigma_0 = \omega'_0 - \underline{k}_0 \cdot \underline{U} \quad (40)$$

and S_0 is the frequency-integrated source function,

$$S_0 = \int_0^{\infty} S(\omega) d\omega \quad (41)$$

The conservation equation (37) can then be written as

$$\frac{\partial}{\partial x}(c'_{x0} \omega'_0 A_0) + \frac{\partial}{\partial y}(c'_{y0} \omega'_0 A_0) + \frac{\partial}{\partial \theta}(c'_{\theta 0} \omega'_0 A_0) \approx \frac{\omega'_0 S_0}{\sigma_0} \quad (42)$$

The righthand side of the conservation equation for determining ω'_0 is thus expressed in terms of integrals over the original source term of the energy balance equation.

Expressions which relate the source function S_0 to wind and bottom parameters are given later in this section.

The righthand side of the conservation equation for A_0 can equally be expressed in terms of integrals over the energy spectrum. From (34) and (42) it can be found that

$$A_0 \frac{d\omega'_0}{dt} = \int \frac{\omega S}{\sigma} d\omega - \omega'_0 \int \frac{S}{\sigma} d\omega \quad (43)$$

from which the source function for A_0 follows as

$$\int \frac{S}{\sigma} d\omega = \frac{S_0}{\sigma_0} - \frac{A_0}{\omega_0} \frac{d\omega'_0}{dt} \quad (44)$$

Since for narrow spectra it seems acceptable to assume

$$\omega'_0 \simeq \omega_0 \quad (45)$$

the conservation equation for A_0 can be written as

$$\frac{\partial}{\partial x}(c'_{x0} A_0) + \frac{\partial}{\partial y}(c'_{y0} A_0) + \frac{\partial}{\partial \theta}(c'_{\theta 0} A_0) \simeq \frac{S_0}{\sigma_0} - \frac{A_0}{\omega_0} \frac{d\omega_0}{dt} \quad (46)$$

In conclusion, the two equations which need to be implemented in the wave hindcast model are equation (42) and (46) to calculate the frequencyintegrated action density A_0 and the mean action frequency ω'_0 , both as a function of x , y and θ . From the values of A_0 and ω'_0 , the corresponding values of E_0 and ω_0 can readily be found with (45) and:

$$E_0 \simeq \sigma_0 A_0 \quad (47)$$

The expressions for the terms in the source functions S_0 and $d\omega_0/dt$ are addressed next.

Source terms

The source term S appearing in the energy balance equation (12) and in the action balance equation (28) represents a number of physical phenomena which add or withdraw energy to or from the wave field. In the parameterization of the action balance equation the source function is supposed to be a given function of the energy density $E(x, y, \omega, \theta)$ and other physical quantities such as wind speed, water depth etc. When S is given in (x, y, ω, θ) -space, then the parameterized source terms S_0 and $d\omega_0/dt$ are readily determined from their definitions, equations (41) and (39).

The evaluation of S_0 and $d\omega_0/dt$ in the hindcast model in accordance with their definitions would require a considerable effort which eventually provides estimates which can also be estimated directly. Information to formulate such direct estimates is available in the literature and with some ad hoc assumptions relatively simple expressions for S_0 and $d\omega_0/dt$ can be obtained.

wind generation

The basic approach to modelling deep water wave generation suggested here is to use relationships between wave parameters and wind as formulated for an ideal situation. This is a fairly conventional approach (e.g. Sanders, 1976; Wilson, 1955; Klatter, 1983).

The ideal situation considered is a limitless ocean over which a constant wind blows since time $t=0$. The development of the total wave energy E_t in time is then approximated with (e.g. Shore Protection Manual, 1973; Wilson, 1955)

$$\tilde{E}_t = a \operatorname{atanh}^d (b \tilde{t}^c) \quad (48)$$

in which

$$\tilde{E}_t = E_t g^2 / U^4 \quad (49)$$

and

$$\tilde{t} = gt/U \quad (50)$$

and

$$E_t = \int_0^{2\pi} E_o(\theta) d\theta \quad (51)$$

The values of the constants a , b , c and d can be determined from information in the literature (e.g. SWAMP, 1982). The rate of change of \tilde{E}_t , expressed in terms of \tilde{E}_t itself is then

$$\left(\frac{d\tilde{E}_t}{d\tilde{t}} \right)_{\text{wind}} = abcd \left(\frac{\tilde{E}_t}{a} \right)^{\frac{d-1}{d}} \left\{ 1 - \left(\frac{\tilde{E}_t}{a} \right)^{\frac{2}{d}} \right\} \left\{ \frac{1}{b} \operatorname{atanh} \left[\left(\frac{\tilde{E}_t}{d} \right)^{\frac{1}{d}} \right] \right\}^{\frac{c-1}{c}} \quad (52)$$

in which atanh denotes the inverse function of tanh .

If the directional distribution of the waves in this ideal situation is assumed to be of the $\cos^2\theta$ -shape, then

$$E_o = B E_t \quad (53)$$

in which

$$\left. \begin{aligned} B &= \frac{2}{\pi} \cos^2(\theta - \theta_w) && \text{for } |\theta - \theta_w| < 90^\circ \\ &= 0 && \text{for } |\theta - \theta_w| \geq 90^\circ \end{aligned} \right\} \quad (54)$$

and θ_w is the wind direction. It follows from (53) that

$$\left(\frac{d}{dt} E_o \right)_{\text{wind}} = B \left(\frac{dE_t}{dt} \right)_{\text{wind}} \quad (55)$$

The rate of change of E_o in terms of E_o itself is then from (52), (53) and (55),

$$\left(\frac{d}{dt} \tilde{E}_o\right)_{\text{wind}} = Babcd \left(\frac{\tilde{E}_o B^{-1}}{a}\right)^{\frac{d-1}{d}} \left\{ 1 - \left(\frac{\tilde{E}_o B^{-1}}{a}\right)^{\frac{2}{d}} \right\} \left\{ \frac{1}{b} \operatorname{atanh} \left[\left(\frac{\tilde{E}_o B^{-1}}{d}\right)^{\frac{1}{d}} \right] \right\}^{\frac{c-1}{c}} \quad (56)$$

in which

$$\tilde{E}_o = B\tilde{E}_t \quad (57)$$

The expression (56) is assumed to be also applicable in non-ideal situations. That is, the instantaneous rate of change of E_o is assumed to be identical to that in an ideal situation with the same wind speed, wind direction and value of E_o as locally and instantaneously defined in the non-ideal situation.

The rate of change of the mean frequency ω_t ,

$$\omega_t = \int_0^{2\pi} \omega_o(\theta) d\theta / 2\pi \quad (58)$$

can be modelled as a function of \tilde{E} :

$$\left(\frac{d\tilde{\omega}_t}{dt}\right)_{\text{wind}} = a_2 \left(\frac{d\tilde{E}_t}{dt}\right)_{\text{wind}}^{b_2} \quad (59)$$

in which

$$\tilde{\omega}_t = \frac{g}{U\omega_t} \quad (60)$$

Since in the ideal situation $\omega_o = \omega_t$ for a $\cos^2 \theta$ directional energy distribution,

$$\left(\frac{d\tilde{\omega}_o}{dt}\right)_{\text{wind}} = a_2 \left(\frac{d\tilde{E}_t}{dt}\right)_{\text{wind}}^{b_2} \quad (61)$$

or, with (57)

$$\left(\frac{d\tilde{\omega}_o}{dt}\right)_{\text{wind}} = a_2 \left\{ \frac{d(\tilde{E}_o B^{-1})}{dt} \right\}_{\text{wind}}^{b_2} \quad (62)$$

The above expressions for E_o and ω_o hold only for growing waves, that is, for values of \tilde{E}_o less than aB . If in the hindcast model refraction or diffraction effects shift the direction of propagation, then the

value of E_0 may obtain a value higher than aB . Changes in E_0 due to changes in the wind do not occur since the wind is constant in the model considered in this study. The wave energy for which $\tilde{E}_0 > aB$ is said to be overdeveloped. In that case it is assumed that E_0 does not change:

$$\left(\frac{dE_0}{dt}\right)_{\text{wind}} = 0 \quad \text{for } E_0 > aB \quad (63)$$

It follows from (61) that ω_0 does also not change in such a case.

Bottom dissipation

The most commonly used approach to model bottom dissipation in hindcast models (e.g. Cavaleri and Rizzoli, 1981; Collins, 1972) is to implement a linearized version of a quadratic bottom friction model combined with estimates of orbital velocities from linear wave theory. Hasselmann and Collins (1968) propose:

$$S_{\text{bottom}}(\omega, \theta) = - \frac{c_f g k c_g}{2\pi\omega^2 \cosh^2(kd)} \langle u \rangle E(\omega, \theta) \quad (64)$$

in which c_g is a friction coefficient and $\langle u \rangle$ is a characteristic value of the wave induced orbital velocity near the bottom. Collins (1972) suggests to use the rms value of the orbital velocities at the bottom as given by linear theory:

$$\langle u \rangle = \left[\int_0^\infty \int_0^{2\pi} \frac{g^2 k^2 E(f, \theta) d f d \theta}{\omega^2 \cosh^2 kd} \right]^{\frac{1}{2}} \quad (65)$$

It would be consistent with the parameterization of the energy balance in terms of E_0 and ω_0 to transform (with some additional assumption) equations (64) and (65) into two dissipation terms for E_0 and ω_0 respectively. A convenient choice would be to replace in equation (63) the frequency dependent variables with their value corresponding to ω_0 :

$$S_{o, \text{bottom}} = \left(\frac{dE_o}{dt} \right)_{\text{bottom}} = - \frac{c_f g k_o c_o}{2\pi \omega_o^2 \cosh(k_o d)} \langle u_o \rangle E_o(\theta) \quad (66)$$

in which

$$\langle u_o \rangle = \int_0^{2\pi} \frac{g^2 k_o^2 E_o}{\omega_o^2 \cosh(k_o d)} d\theta \quad (67)$$

The situation as regards the corresponding bottom-induced rate of change of $\omega_o(\theta)$ is not so obvious. In fact, the state-of-the-art on this subject (SWIM, 1983) is confusing in the sense that recent observations indicate that the value of ω_t is hardly affected by bottom dissipation while most of the other available information indicates that it is affected. A prudent approach is therefore advised. A simple and flexible model would be to relate the rate of change of $\omega_o(\theta)$ directly to the rate of change of $E_o(\theta)$:

$$\left(\frac{d\omega_o}{dt} \right)_{\text{bottom}} = \omega_o^2 a_3 \left\{ g^{-2} \omega_o^3 \left(\frac{dE_o}{dt} \right)_{\text{bottom}} \right\}^{b_3} \quad (68)$$

in which a_3 and b_3 are dimensionless coefficients to be determined empirically (e.g. with observations in the Oosterschelde area).

Surf dissipation

A model which seems to provide reasonable estimates of wave energy dissipation in the surfzone is due to Battjes and Janssen (1978). The energy dissipation in this model is based on an assumed similarity between the dissipation in a breaking wave and that in a bore. It can only be used to estimate the total dissipation,

$$\left(\frac{dE_t}{dt} \right)_{\text{surf}} = \alpha_1 \frac{\pi}{2} Q_b \omega_t^2 g H_m^2 \quad (69)$$

in which α_1 is a constant of the order 1, Q_b is the fraction of breaking waves (of the total local population of waves) and H_m is the local maximum wave height. The value of Q_b is determined from a Rayleigh distribution truncated at H_m

$$\frac{1-Q_b}{\ln Q_b} = - 8 \frac{E_t}{H_m^2} \quad (70)$$

in which H_m can be estimated as

$$H_m = 0.88 k_o^{-1} \tanh(\gamma k_o d / 0.88) \quad (71)$$

To estimate from (69) the corresponding rate of change of E_o and ω_o , some ad hoc assumptions are required as regards the effects of this dissipation on ω_o and also as regards the directional distribution of this dissipation. Considering the observation reported in section 4 on the apparent lack of interaction between crossing breakers, one might assume the surf dissipation to be directionally distributed as the energy density E_o ,

$$\left(\frac{dE_o}{dt}\right)_{\text{surf}} = \alpha_1 \frac{\pi Q_b \omega_t \rho g H_m^2 E_o}{2 E_t} \quad (72)$$

For the rate of change of ω_o , the best assumption at present is perhaps a simple relationship,

$$\left(\frac{d\omega_o}{dt}\right)_{\text{surf}} = \omega_o^2 a_4 \left\{ g^{-2} \omega_o^3 \left(\frac{dE_o}{dt}\right)_{\text{surf}} \right\}^{b_4} \quad (73)$$

Perhaps that results of the calibration of CREDIZ for applications in the Haringvliet can provide estimates for a_4 and b_4 .

Currents

The effect of currents on wind generation is taken into account by replacing in the relevant expressions the wind relative to a fixed frame of reference (fixed to the bottom topography) by a wind relative to the local current (vector subtraction).

The effect of currents on bottom dissipation and surf dissipation is ignored until evidence is submitted that this is not justifiable.

5.2 Numerical formulation

The basic equations which need to be implemented numerically in the wave hindcast model are the balance equations (42) and (46) to determine the frequency-integrated action A_0 and the mean action frequency ω'_0 . These equations contain variables and gradients which are defined in three dimensions: x , y and θ . The computations should therefore also be carried out in three dimensions. However, the implementation of a model to carry out such computations would require a substantial effort and the CPU-time for operational applications would be high. It is therefore recommended to reduce the number of dimensions to two in a manner similar to the one which has been used in the development of CREDIZ.

In CREDIZ a parabolic version of the elliptic mild slope equation (13) has been implemented. This approximation of an elliptic equation by a parabolic equation opened the possibility of reducing the computational effort considerably. This approximation was permitted under the condition that all wave energy propagates in a narrow directional sector around the computational direction which should be chosen roughly equal to the average wave direction. The computation can then be carried out line by line progressing in the computational direction.

A similar approach is taken in the implementation at the present hindcast model. The computation progresses in one direction, called x -direction, and the wave condition in each point is computed explicitly. In contrast with the mild-slope equation no approximations are necessary. The only limitation is that only waves with directions in a certain sector are considered (see fig. 11).

The numerical method which is recommended here to obtain a solution to the two basic conservation equations of the model is an explicit predictor-corrector scheme. This scheme is preferred over an implicit scheme for the following reasons:

- (a) an explicit scheme requires less programming effort than does an implicit scheme
- (b) source terms in the conservation equations are more readily modified in an explicit scheme than in an implicit scheme
- (c) the source terms are strongly nonlinear, so that many iterations would be required in an implicit method, which destroys any computational advantages of that method.

The predictor-corrector scheme proposed below allows for an arbitrary number of corrector steps. One predictor step and one corrector step is probably adequate for the expected applications of the hindcast model. The computations are carried out line by line progressing in the x-direction (the computational direction); the aforementioned lines are parallel to the y-axis, which is normal to the x-axis (see fig. 11). The numerical procedure can be formulated in terms of the derivatives along the x-axis as a function of the other derivatives and the source terms appearing in the conservation equations.

For brevity of notation each of the basic conservation equations is written in a compact form as:

$$\frac{\partial a_i F_i}{\partial x} = f_i(F_1, \dots, F_N; G_1, \dots, G_N) - n_i F_i \quad i=1, \dots, N \quad (74)$$

$$\frac{\partial a_i G_i}{\partial x} = g_i(F_1, \dots, F_N; G_1, \dots, G_N) - m_i G_i \quad i=1, \dots, N \quad (75)$$

in which F_i is A_o and G_i is $\omega_o' A_o$ at numbered locations (number i) in the (y, θ) -plane, a_i are the corresponding propagation speed c_x . The nonlinear terms of the conservation equations and the derivatives of A_o or $\omega_o' A_o$ with respect to y and θ are incorporated in f_i and g_i . The linear terms are represented by $n_i F_i$ and $m_i G_i$. The integration in x-direction of the conservation is carried out with a central difference scheme which for equation (74) is:

$$\frac{a_i^{m+1} F_i^{m+1} - a_i^m F_i^m}{\Delta x} = f_i(F_1^{m+\frac{1}{2}}, \dots, F_N^{m+\frac{1}{2}}; G_1^{m+\frac{1}{2}}, \dots, G_N^{m+\frac{1}{2}}) - n_i \left(\frac{F_i^m + F_i^{m+1}}{2} \right) \quad (76)$$

in which m refers to the position in the x-domain. It follows that

$$F_i^{m+1} = \frac{a_i^m F_i^m - \frac{1}{2} \Delta x \cdot n_i F_i^m + \Delta x \cdot f_i(F_1^m, \dots, F_N^m; G_1^m, \dots, G_N^m)}{a_i^{m+1} + \frac{1}{2} \Delta x \cdot n_i} \quad (77)$$

In the predictor step $F_i^{m+\frac{1}{2}}$ is taken equal to F_i^m , in the corrector step(s) $F_i^{m+\frac{1}{2}}$ is taken equal to $\frac{1}{2}(F_i^m + F_i^{m+1})$. An identical scheme should be used for G_i . The procedures can be repeated for as many corrector steps as desired but it seems sufficient for the present model to use only one predictor and one corrector step.

To ensure that the numerical scheme is conservative (conservation of the propagated property apart from sources and sinks), the numerical representation of the derivatives in the conservation equations should be conservative. This is true for the above scheme as far as $\partial a_i F_i / \partial x$ is concerned. The transportation terms in (y, θ) -space which are incorporated in f_i and g_i can also be represented in a conservative finite difference scheme. Denoting the location in y-space with j and the location in θ -space with k, the following scheme is suggested:

$$\frac{\partial T_y}{\partial y} + \frac{\partial T_\theta}{\partial \theta} \approx \frac{T_{y, j+\frac{1}{2}, k}^m - T_{y, j-\frac{1}{2}, k}^m}{\Delta y} + \frac{T_{\theta, j, k+\frac{1}{2}}^m - T_{\theta, j, k-\frac{1}{2}}^m}{\Delta \theta} \quad (78)$$

in which T_y and T_θ are the fluxes in y- and θ -space respectively. The value of T_y at the intermediate location $j+\frac{1}{2}$ can be determined from the surrounding position j and j+1 as

$$T_{y, j+\frac{1}{2}, k}^m = \frac{1}{2}(T_{y, j, k}^m + T_{y, j+1, k}^m) \quad (79)$$

The other values in (78) of T_y and T_θ are obtained in a similar fashion. The condition that all energy should travel in a directional sector around the fixed direction (of the positive x-axis) implies that

energy propagating from this sector to directions outside this sector disappears from the model (absorbed by the boundaries in the θ -space). It is also assumed that no energy enters the model from directions outside the specified sector. Similar conditions hold for the boundaries of the model in y -direction (fig. 11).

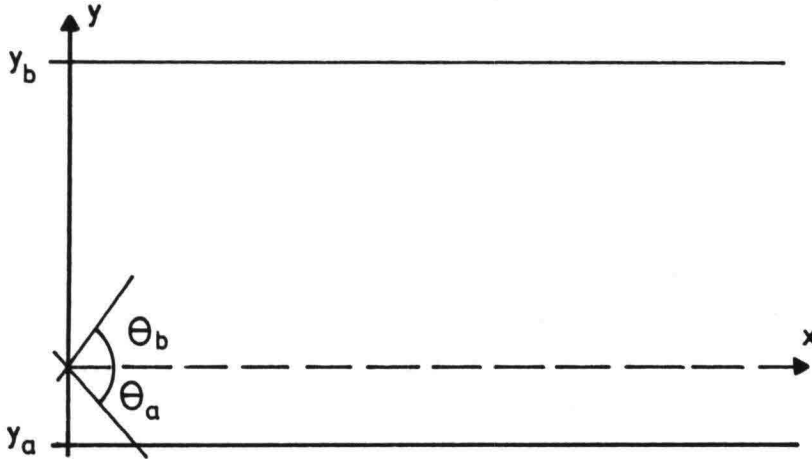


Figure 11: The computational region.

Derivatives of higher order than the first in the conservation equations are neglected at the boundaries in (y, θ) -space; refraction terms are retained.

6. CONCLUSION

The basic characteristics for a numerical wave hindcast model for the Oosterschelde has been formulated. This model is expected to provide realistic estimates of wave conditions within rather severe operational constraints. It can be characterized as a directionally decoupled, parametric model. For each of a number of spectral wave directions the wave energy density and a mean wave frequency are determined with a model that represents wave propagation, generation and dissipation.

The propagation part of the model includes conventional refraction of the parameterized wave energy spectrum and some degree of diffraction. A fundamentally correct suggestion has been made to include diffraction but its implementation does not seem to be feasible. Alternative suggestions of a more pragmatic nature have been added.

The generation and dissipation parts of the model are fairly conventional but some ad hoc choices were made. These choices need to be further investigated with the help of observations, preferably in the Oosterschelde.

REFERENCES

- Battjes, J.A. (1968), Refraction of water waves, Journal of the Waterways and Harbors Division, ASCE, Vol. 94, No. WW4, Proc. Paper 6206, Nov. 1968, pp. 437-451.
- Battjes, J.A. and J.P.F.M. Jansen (1978), Energy loss and set-up due to breaking of random waves, Proc. 16th Coastal Engineering Conference, Hamburg, publ.: ASCE, New York, pp. 569-587.
- Berkhoff, J.C.W. (1976), Mathematical models for simple harmonic linear water waves, report on mathematical investigation, Delft Hydr. Lab., Report W 154-IV.
- Booij, N. (1981), Gravity waves on water with non-uniform depth and current. Communications on Hydraulics, report no. 81-1, Delft Univ. Techn., Dept. of Civil. Engineering.
- Booij, N. and A.C. Radder (1981), CREDIZ: a refraction-diffraction model for sea waves. Divisie 1981 E, Rijkswaterstaat, Data Processing Division.
- Bretherton, F.P. and C.J.R. Garrett (1969), Wavetrains in inhomogeneous moving media, Proc. Roy. Soc., A, vol. 132, pp. 529-554.
- Cavaleri, L. and Malanotte Rizzoli, P. (1981), Wind wave prediction in shallow water: theory and applications, Journal of Geophysical Research, Vol. 86, No. c11, pp. 10961-10973, Nov. 20.
- Collins, J.I. (1972), Prediction of shallow water spectra, Journal of Geophysical Research, Vol. 77, No. 15, pp. 2693-2707.
- Hasselmann, K. and J.I. Collins (1968), Spectral dissipation of finite depth gravity waves due to bottom friction, Journal of Marine Research, Vol. 26. No. 1, pp. 1-12.

- Hasselmann, K. (1968), Weak-interaction theory of ocean waves, In: Basic developments in fluid dynamics, Vol. 2, M. Holt (ed.), New York, Academic Press, pp. 117-182.
- Hasselmann, K. et al. (1973), Measurements of wind-wave growth and swell decay during the Joint North Sea Wave Project (JONSWAP), Ergänzungsheft zur Deutschen Hydrographischen Zeitschrift, Reihe A (8), No. 12.
- Houmb, O.G. and T. Overvik (1976), Parameterization of wave spectra and long term joint distribution of wave height and period, Proc. BOSS '76, Int. Conf. Behaviour of Off-Shore Structures, Trondheim, Vol. 1, Norwegian Institute of Techn. 144-169.
- Klatter, H.E. (1983), Een tweeparameter golfvoorspellingsmodel (A two-parameter wave prediction model), Master thesis in Dutch, R-1983/5/H, Group of Fluid Mechanics, Department of Civil Engineering, Delft University of Technology.
- Sanders, J.W. (1976), A growth-stage scaling model for the wind-driven sea, Deutsches Hydrographisches Zeitschrift, Vol. 29, pp. 136-161.
- Schönfeld, J.Ch. (1972), Voortplanting van korte golven in twee dimensies (Propagation of short-period waves in two dimensions), manuscript in Dutch, Dept. of Civil Engineering, Delft University of Technology.
- Shore Protection Manual (1973), U.S. Army Coastal Engineering Research Centre, Corps of Engineers.
- SWAMP (1982), The Sea Wave Modelling Project, draft for the Proceedings, Conference on Radio Probing and Wave Dynamics of the Ocean, Miami, 1981.

SWIM, Shallow water intercomparison of wave prediction models, personal communications, project of the British Meteorological Office (Bracknell), the Max Planck Institut für Meteorologie (Hamburg) and the Koninklijk Nederlands Meteorologisch Instituut (de Bilt).

Whitham, G.B. (1971), Dispersive waves and variational principles. In: Studies of Applied Mathematics, ed. by A.H. Taub, pp. 181-212. Math. Ass. of America.

Whitham, G.B. (1974), Linear and nonlinear waves, sec. 7.7. Publ.: Wiley, New York.

Wilson, B.W. (1955), Graphical approach to the forecasting of waves in moving fetches, Beach Erosion Board, Corps of Engineers, Department of the Army, Techn. Memo. 73.

APPENDIX 1

In this preliminary investigation refraction calculations have been carried out for a rectangular area over the "Oosterschelde" containing the "Galgeplaat". In this appendix results of these computations for a water level at NAP are presented.

In figures 1-10 rays are plotted for all combinations of wave periods 1.5 s and 3 s and directions of wave propagation WSW, WNW, NW, NNW, NNE (or, more precisely, 255° (30°) 15° , nautical convention).

The rectangular area in figures 1-10 corresponds to the bottom plot on page 6. For convenience bottom contours are plotted at depth intervals of 10 m. A number of equidistant (100-200 m) and parallel rays start from the boundary of the area considered but only where the bottom at that boundary is below water level. The rays are marked every 20 wave lengths.

DATE: 83/10/24
TIME: 15 20 10
DSN: UJUNTHC
REFRAI
PICT: 6
SCALE: 6

END OF FILE FOUND
ENTER ONE OF NEXT
3 POSSIBILITIES.
PICT() SCALE()
DISCARD
HOLD

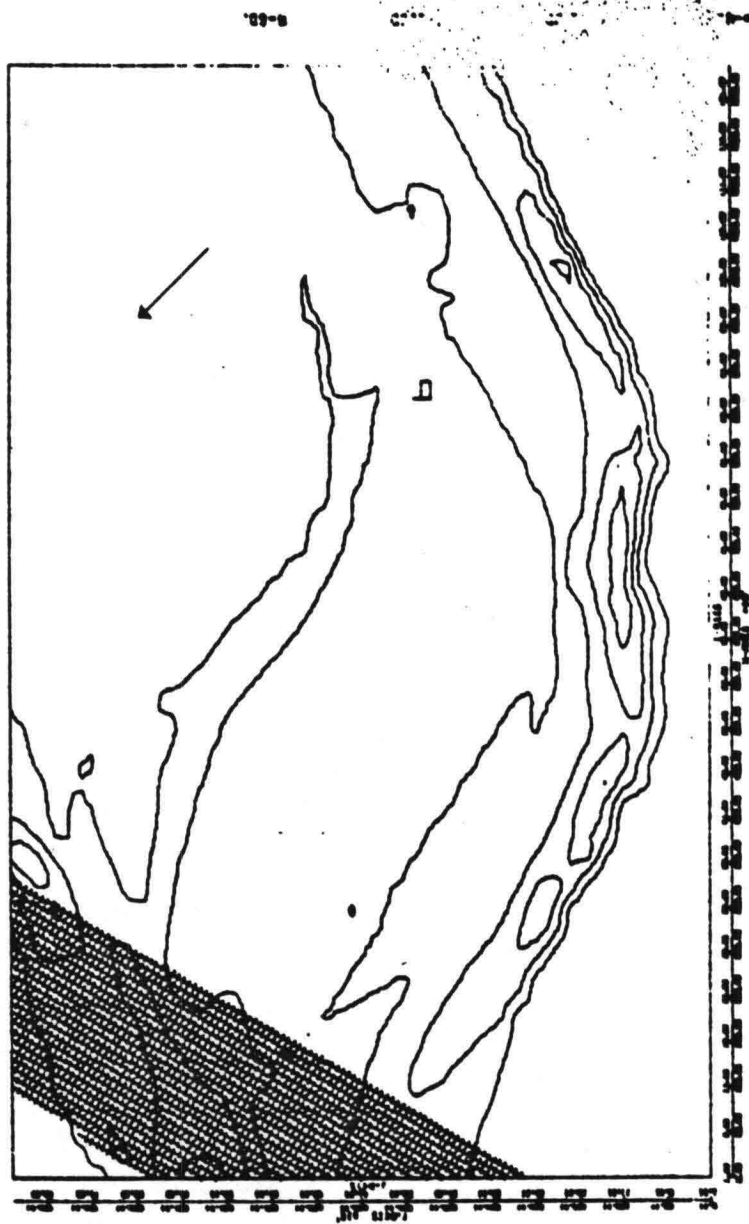


Figure 1:
water level NAP
wave period 1.5 s
wave direction 255°

DATE: 83/10/24
TIME: 15 29 58
DSN: WUUMTHC
REFRA3
PICT: 1
SCALE: 6

PICTURE ENDED
ENTER ONE OF NEXT
3 POSSIBILITIES
PICT() SCALE()
DISCARD
HOLD

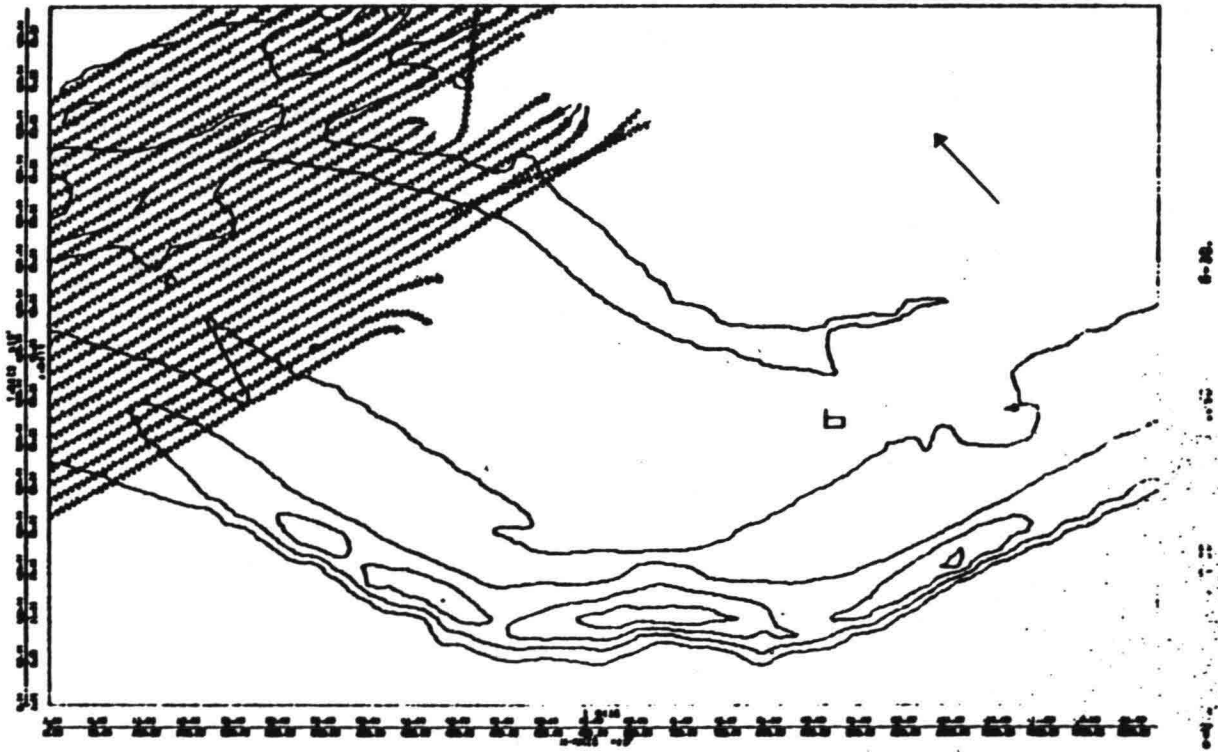


Figure 2:
water level NAP
wave period 1.5 s
wave direction 285°

DATE 83/10/24
TIME 15 57 31
DSN UJURTHC
REFRA3
PICT 2
SCALE 6

PICTURE ENDED
ENTER ONE OF NEXT
3 POSSIBILITIES.
PICT() SCALE()
DISCARD
HOLD

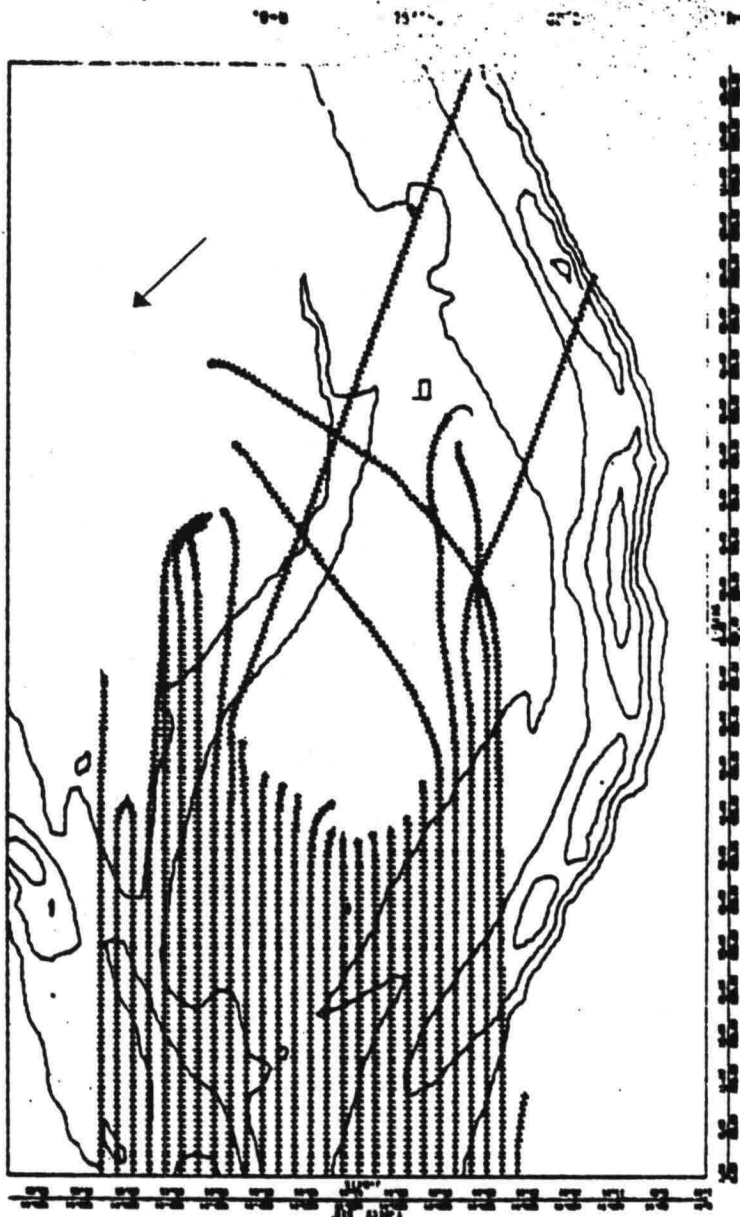


Figure 3:
water level NAP
wave period 1.5 s
wave direction 315°

DATE: 83/10/24
TIME: 16 08 56
DSN: UJURTHC
REFRA4
PICT: 1
SCALE: .6

PICTURE ENDED
ENTER ONE OF NEXT
3 POSSIBILITIES:
PICT() SCALE()
DISCARD
HOLD

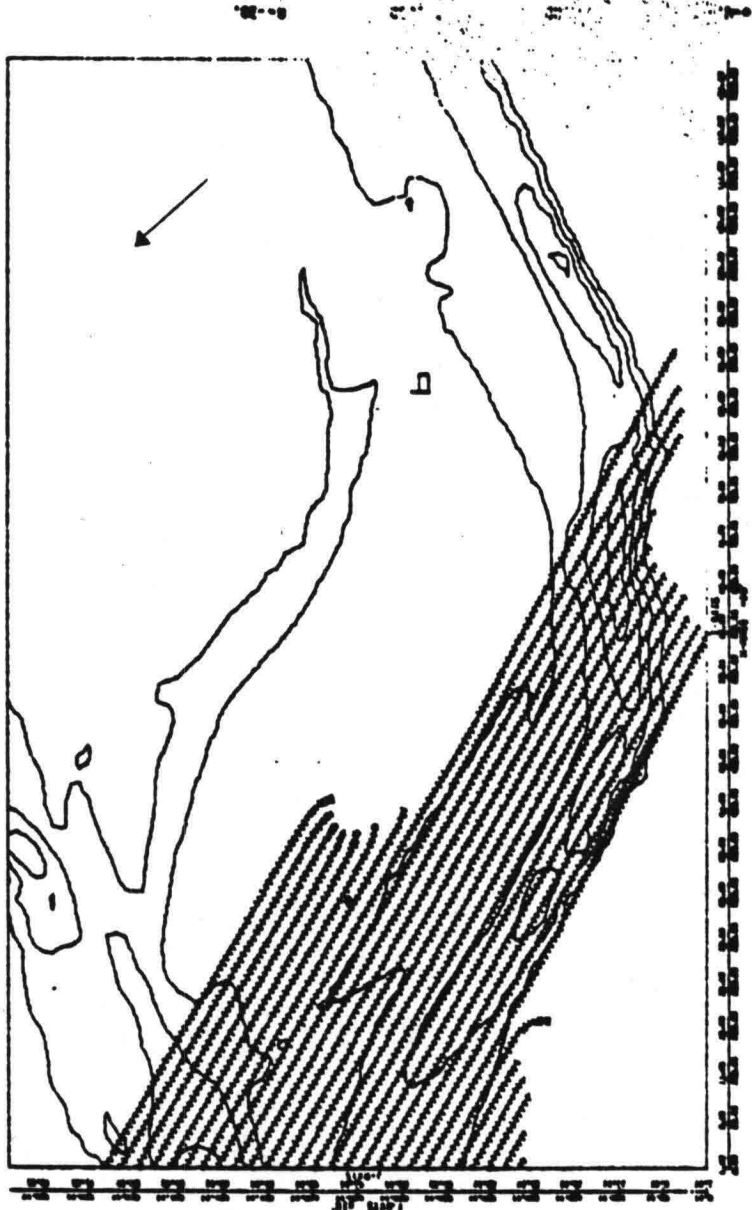


Figure 4:
water level NAP
wave period 1.5 s
wave direction 345°

DATE: 83/10/24
TIME: 16 20 01
DSN: UNJNTHC
REFRA: 2
PICT: 2
SCALE: .6

PICTURE ENDED
ENTER ONE OF NEXT
3 POSSIBILITIES
PICT() SCALE()
DISCARD
HOLD

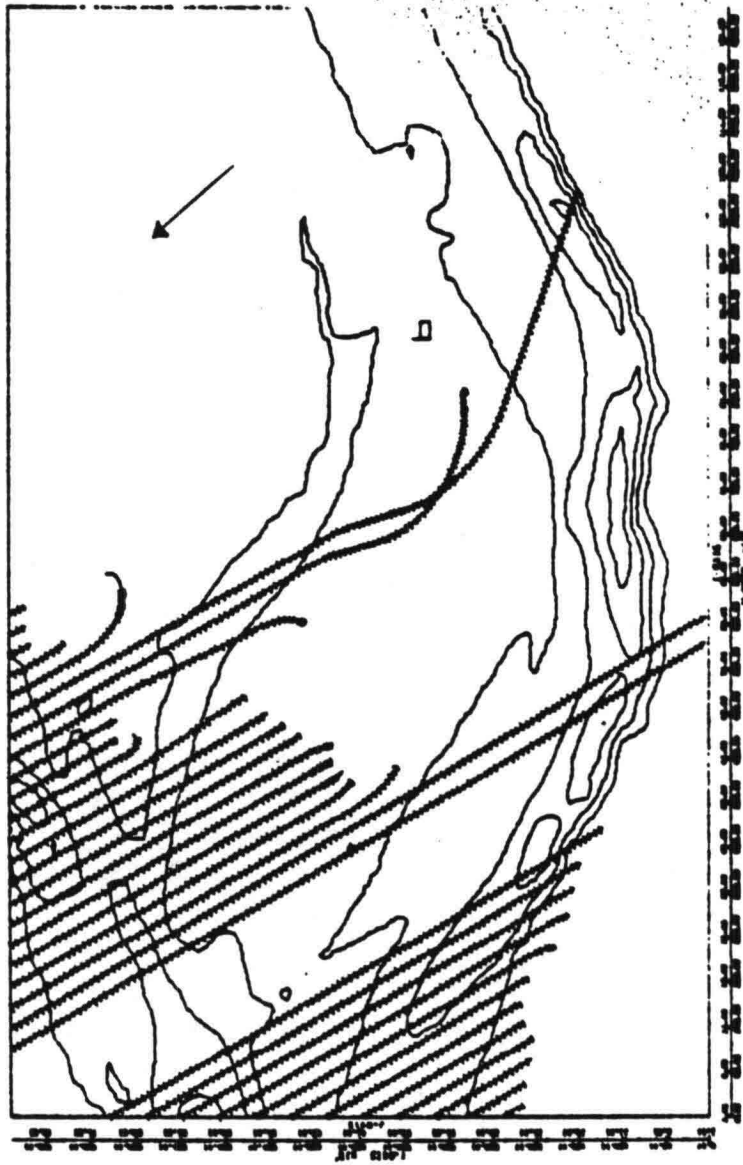
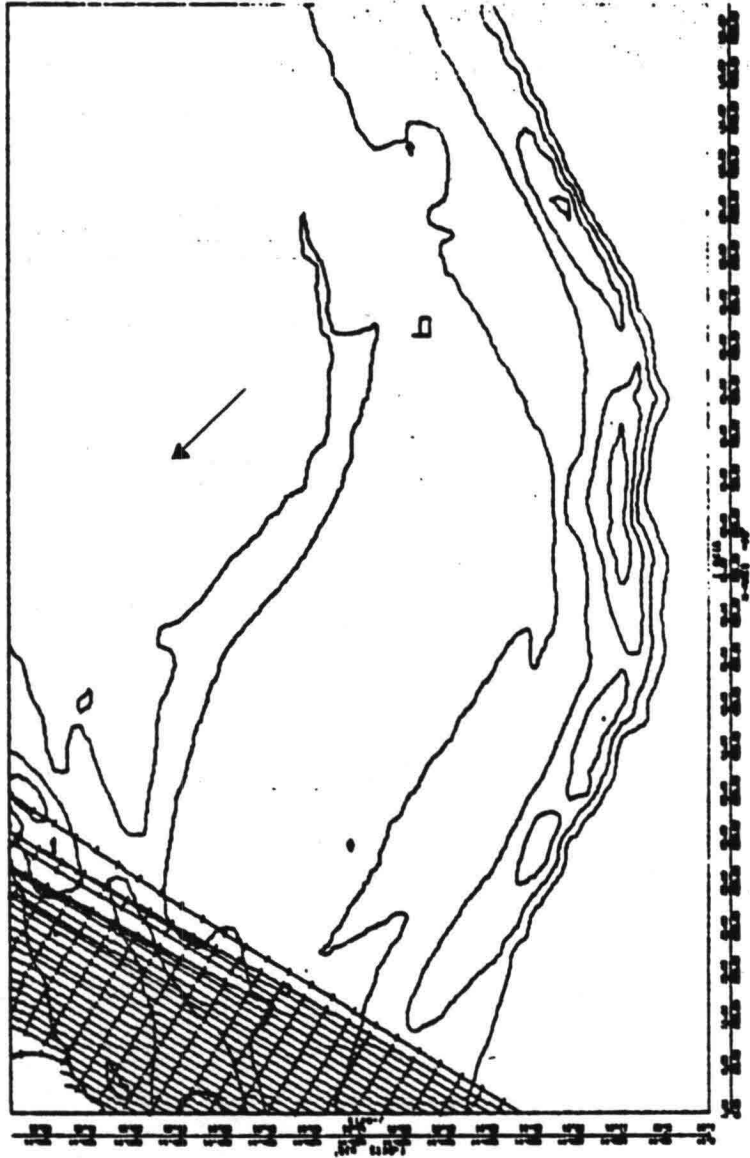


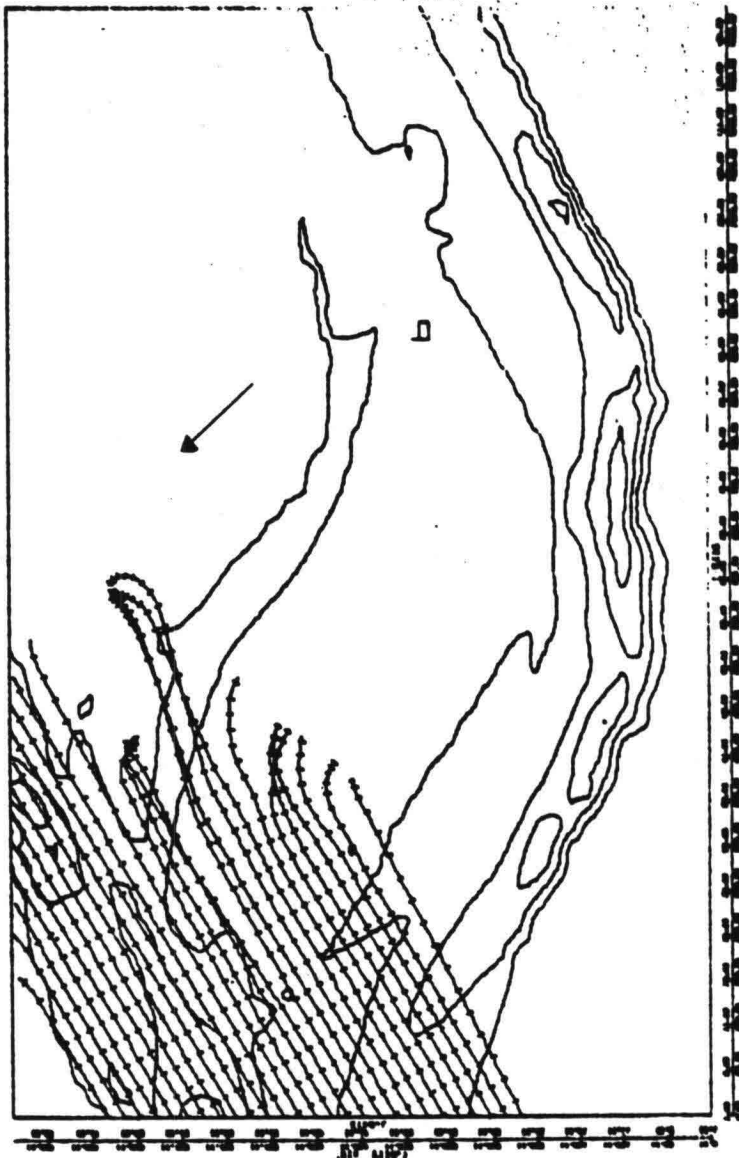
Figure 5:
water level NAP
wave period 1.5 s
wave direction 15°



DATE: 83/10/24
TIME: 14.34.52
DSN: UJWTHC
REFRAI
PICT: 1
SCALE: .6

PICTURE ENDED
ENTER ONE OF NEXT
3 POSSIBILITIES.
PICT() SCALE()
DISCARD
HOLD

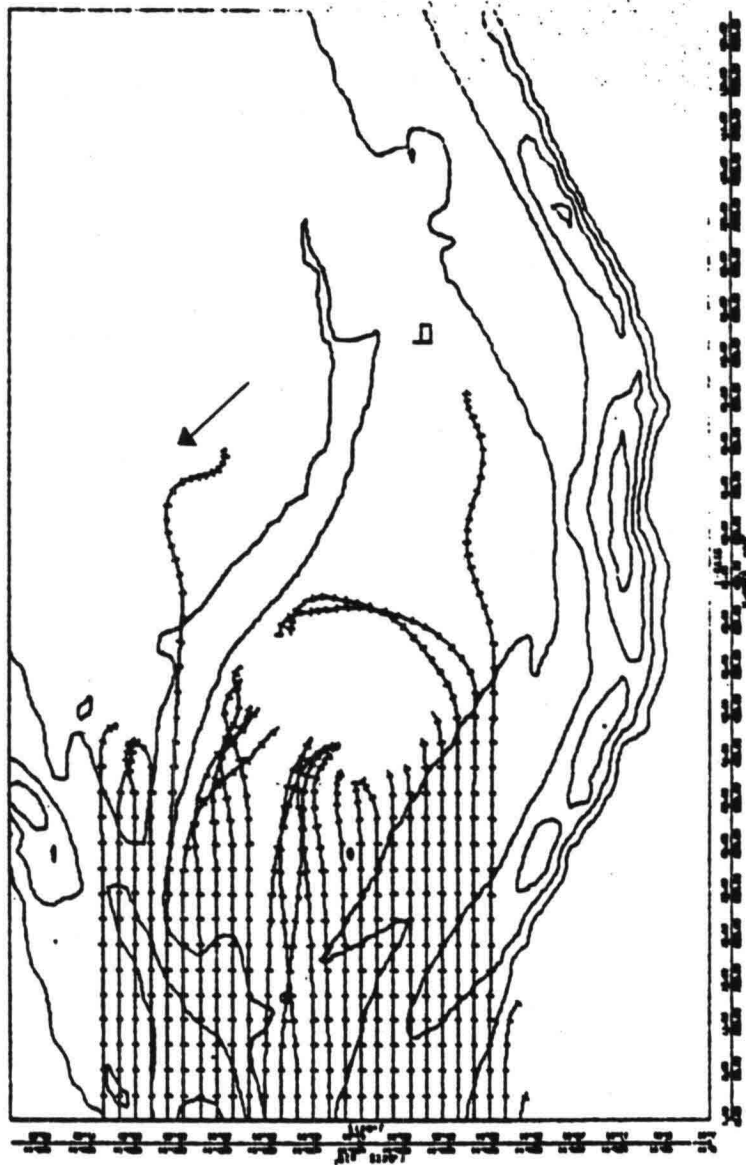
Figure 6:
water level NAP
wave period 3.0 s
wave direction 255°



DATE: 83/10/24
TIME: 14 43 33
DSN: UUNRTHC
REFPAL
PICT: 2
SCALE: 6

PICTURE ENDED
ENTER ONE OF NEXT
3 POSSIBILITIES.
PICT() SCALE()
DISCARD
HOLD

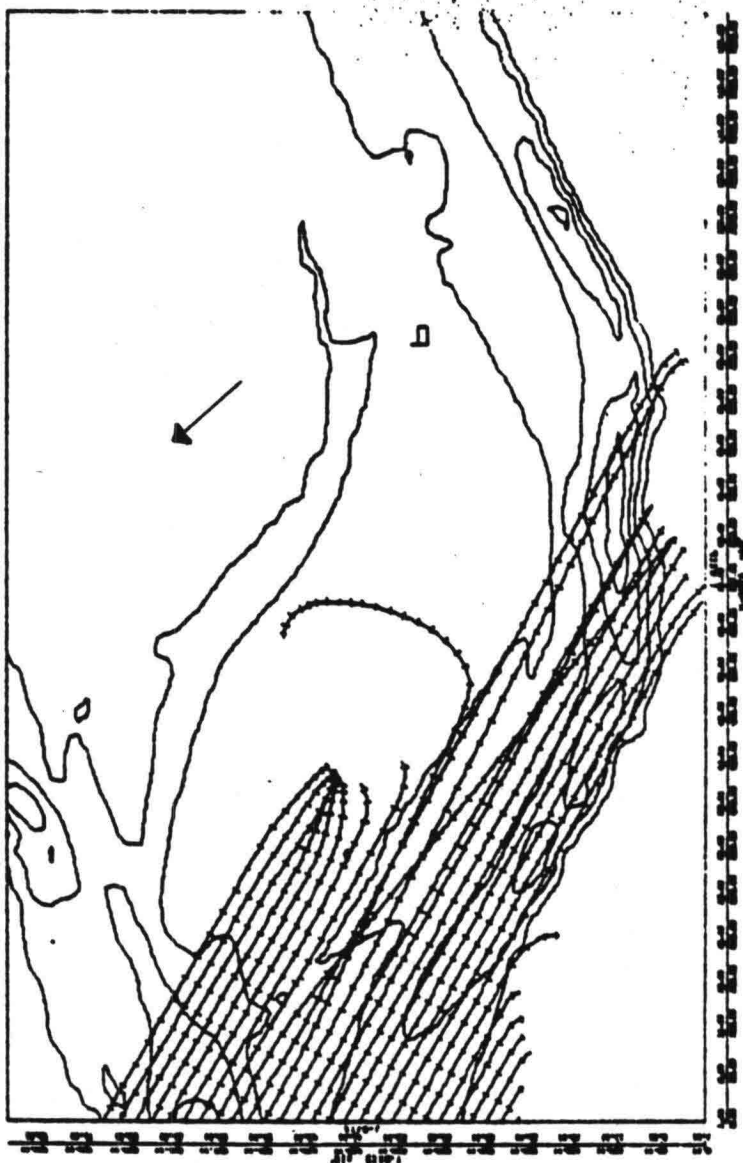
Figure 7:
water level NAP
wave period 3.0 s
wave direction 285°



DATE: 83/10/24
TIME: 14:51:34
DSN: WJUMTHC
REFRA1
PICT: 3
SCALE: 6

PICTURE ENDED
ENTER ONE OF NEXT
3 POSSIBILITIES
PICT() SCALE()
DISCARD
HOLD

Figure 8:
water level NAP
wave period 3.0 s
wave direction 315°



DATE: 83/10/24
TIME: 15.04.45
DSN: UURMTHC
REFRA1
PICT: 4
SCALE: .6

PICTURE ENDED
ENTER ONE OF NEXT
3 POSSIBILITIES
PICT() SCALE()
DISCARD
HOLD

Figure 9:
water level NAP
wave period 3.0 s
wave direction 345°

DATE: 83/10/24
TIME 15.12.58
DSN UNJUTHC
REFRA1
PICT 5
SCALE 6

PICTURE ENDED
ENTER ONE OF NEXT
3 POSSIBILITIES.
PICT() SCALE()
DISCARD
HOLD

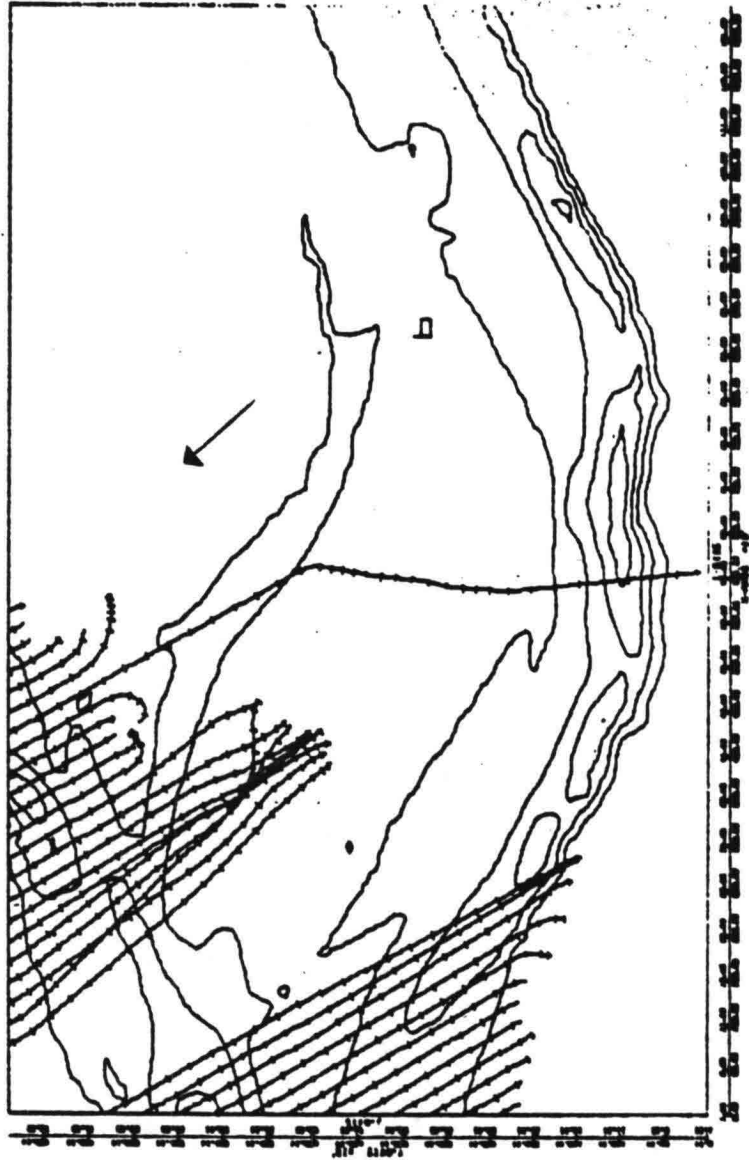


Figure 10:
water level NAP
wave period 3.0 s
wave direction 15°

